

N64-17680

CODE-1

CB-55973

RE-170

ASTRODYNAMICS OF LUNAR

SATELLITES:

PART II - LUNAR ORBIT STABILITY

November 1963

Grumman

RESEARCH DEPARTMENT

OTS PRICE

XEROX

\$

6.60 per

MICROFILM

\$

2.06 ref.

GRUMMAN AIRCRAFT ENGINEERING CORPORATION

BETHPAGE NEW YORK

(NASA CR - 55973;)
Grumman Research Department Report RE-170

OTS: 46.60 ph,
4 2.06

1082072 Grumman Aircraft
Engineering Corp., Bethpage, N.Y.
② Research Dept.

ASTRODYNAMICS OF LUNAR SATELLITES 24
PART II: LUNAR ORBIT STABILITY

by 1(2) Final Report

(G. Pinkham
and
F. Sobierajski)
Systems Research

November 1963 62 p ef

Final Report (NASA)
on Contract NAS(8-5015)
Aero-Astroynamics Laboratory
Marshall Space Flight Center
National Aeronautics and Space Administration
Huntsville, Alabama

Approved by: Charles E. Mack, Jr.
Charles E. Mack, Jr.
Director of Research

504-13341

ABSTRACT

17680

A ?

This report presents the conclusions reached in Part II in the course of investigating the "Astrodynamics of Lunar Satellites" under Contract NAS 8-5015. The work was done by the Grumman Research Department, Bethpage, N.Y. under the auspices of NASA's Marshall Space Flight Center, Aero-Astrodynamics Laboratory, Flight Evaluation Branch.

The purpose of this part of the contract was to study the stability of lunar satellites perturbed by the moon's triaxial potential and by the attractions of the earth, sun, and planets. An approximate analytic solution for the motion of a lunar satellite was derived and extensive numerical studies were performed.

This report contains the conclusions and data from these studies. The body of the report includes the main conclusions and a portion of the data; and the appendices contain the derivations, equations, and additional data.

Author

TABLE OF CONTENTS

<u>Item</u>	<u>Page</u>
Introduction	1
The Approximate Solution	2
Background and Description of Derivation	2
Solution and Main Conclusions	3
Numerical Study	6
Explanation of Graphs and Tables	6
The Plan of Computation	8
Conclusions	9
Recommendations for Future Study	12
References	13
Appendix A - The Average Motion of a Lunar Satellite	31
Appendix B - A Variation-of-Parameters Scheme for Lunar Orbits	40
Appendix C - Catalog of Numerical Results	49

LIST OF ILLUSTRATIONS

<u>Figure</u>		<u>Page</u>
1	Schematic of Earth, Moon, and Sun Configurations at Three Epochs	18
2-5	Lunar Satellite Orbits Perturbed by Earth, Moon, Sun, and Planets at 9 January 1969	19-22
6-9	Lunar Satellite Orbits Perturbed only by the Triaxial Moon	23-26
10-13	Eccentric Lunar Satellite Orbit Perturbed by the Earth, Moon, Sun, and Planets at 9 January 1969	27-30

LIST OF TABLES

<u>Table</u>		<u>Page</u>
1	Initial Orbital Parameters for Figs. 2 through 13	14
2	Perturbations of Lunar Orbits at 9 January 1969	15
3	Perturbations of Lunar Orbits Due to the Moon Only	15
4	Perturbations of Lunar Orbits at 17 December 1963	16
5	Perturbations of Lunar Orbits at 5 January 1960	16
6	Variation in Position Due to Variation in the Astronomical Unit	17
7	Variation in Position Due to Variation in the Principal Axes of the Moon	17
8	Schedule of Inputs	50
9	Perturbations of Lunar Orbits at 9 January 1969 Circular Orbits Perturbed by the Moon, Earth, Sun, and Planets	52
10	Perturbations of Lunar Orbits at 9 January 1969 Eccentric Orbits Perturbed by the Moon, Earth, Sun, and Planets	52
11	Perturbations of Lunar Orbits at 9 January 1969 Circular Orbits Perturbed by the Moon and Earth	53
12	Perturbations of Lunar Orbits at 9 January 1969 Circular and Eccentric Orbits Perturbed Only by the Aspherical Moon	53

LIST OF SYMBOLS

a	}	classical elements of the lunar satellite orbit with respect to inertial reference
e		
i		
ω		
Ω		
T		
a_j		j^{th} direction cosine of satellite radius vector
b_j		length of j^{th} principal axis of lunar ellipsoid; $b_1 > b_2 > b_3 > 0$
B_4		$b_1^2 + b_2^2 + b_3^2$
h		$\sqrt{k_m a(1 - e^2)}$
h_z		$h \cos i$
k_E		gravitational constant of the earth
k_S		gravitational constant of the sun
k_m		gravitational constant of the moon
R		disturbing function
\tilde{R}		approximation to R
$\langle \tilde{R} \rangle$		average of \tilde{R} over a satellite revolution
\bar{R}		$\langle \tilde{R} \rangle + \delta_E h_z$
R_p		small eccentricity approximation to \bar{R}

r	satellite radius
r_E	earth-moon distance (assumed constant)
r_S	sun-moon distance (assumed constant)
S_1	angle between earth-moon line and satellite radius vector
S_2	angle between sun-moon line and satellite radius vector
α_1	$\sqrt{k_m a}$
α_2	h
α_3	h_z
β_1	$\sqrt{k_m/a^3} T = nT$
β_2	$-\omega$
β_3	$-\Omega$
γ	$\Omega - \delta_E t$, angle of line of nodes of satellite orbit with respect to the earth-moon line
δ_E	angular velocity of the earth about the moon
δ_S	angular velocity of the sun about the moon
Λ	constant of the moon potential
ϕ_E	$\delta_E t$, angle of earth-moon line in inertial reference
ϕ_S	$\delta_S t$, angle of sun-moon line in inertial reference
i_E	angle of inclination measured from the earth equatorial plane

a canonical set of orbital elements with potential function \bar{R}

u	radial velocity
w	circumferential velocity
Ω_E	angle of line of nodes measured in the earth equatorial plane
ω_E	angle of periselenium measured from Ω_E
Δr	difference between maximum and minimum radius throughout orbit
Δa	difference between maximum and minimum a throughout orbit
Δa_m	difference between maximum and minimum mean value of a throughout orbit
e_{\max}	maximum value attained by the eccentricity throughout orbit
Δi_e	difference between maximum and minimum values of i_E
$\Delta \Omega_E$	difference between maximum and minimum values of Ω_E
ϕ	a linear function of time

INTRODUCTION

The second part of this contract examines the stability of lunar satellites. Two avenues of approach have been used. The first is based on a technique in nonlinear differential equations known as the Kryloff-Bogoliuboff averaging process. Using this technique on near circular lunar orbits makes it possible to derive an approximate solution to the equations of motion which describe the long term behavior of these orbits. The second approach is purely a numerical one based on a high precision variation of parameters integration routine. With this, a survey has been made of the perturbations of lunar satellite orbits with many different initial conditions and at different times during the 18 year lunar cycle.

The first section of this second part of the final report describes the Kryloff-Bogoliuboff averaging process and the principal results obtained from it for lunar satellite orbits. Also included are comparisons between numerical and approximate analytic solutions. The second section describes the numerical study and includes graphs and tables of the principal results. The appendices contain the actual derivation of the approximate solution, the equations upon which the integration routine is based, and a thorough catalog of the numerical results.

THE APPROXIMATE SOLUTION

Background and Description of Derivation

The Kryloff-Bogoliuboff averaging process is a powerful tool for analyzing the long term behavior of some mechanical systems, and it is based upon the following observations. Let there be given a system of differential equations of the form

$$\frac{dx}{dt} = \mu f(x, t), \quad (1)$$

where μ is small, and f is periodic in t with period P . Expanding f in a Fourier series in t allows the equation to be written as

$$\frac{dx}{dt} = \mu f_0(x) + \mu \sum_{n=1}^{\infty} f_n(x) \cos\left(\frac{2n\pi}{P} t\right) \quad (2)$$

If μ is sufficiently small, the quantities x will change slowly, and the integral

$$\mu \int_0^P \sum_{n=1}^{\infty} f_n \cos\left(\frac{2n\pi}{P} t\right) dt \approx 0 \quad (3)$$

will contribute very little to x over any one cycle. Therefore, to examine the long term behavior, or secular changes, in x the system of equations

$$\frac{dx}{dt} = \mu f_0(x) \quad (4)$$

may be studied in place of the original. Because

$$f_0(x) = \frac{1}{P} \int_0^P f(x, t) dt \quad (5)$$

Research Dept.
RE-170
November 1963

Equations (4) are called the averaged equations. If f is nonlinear, the new system will, in all likelihood, be nonlinear as well. But it will be autonomous and generally simpler. Reference 1 contains a general description of this method and Ref. 2 is an application to lunar orbits. Reference 2, however, obtains only a first integral and employs an angle as independent variable rather than the time.

The differential equations describing the behavior of a lunar satellite orbit may be given the desired form if the parameters of the orbit are chosen as state variables and some simplifications are made. The principal assumptions which must be made are that the moon revolves about the earth in a fixed circular orbit and that the moon rotates in this same orbital plane always keeping its longest principal axis pointed toward the earth. With this model, the perturbations which may be included are those due to the triaxial moon, and a point mass earth and sun. But replacing the original equations with the averaged set does not immediately produce a system which can be solved unless the further assumption of negligible eccentricity in the satellite orbit is made. When this is done, however, the entire problem may be solved by quadratures. The parameters which are used to describe the orbit and in terms of which the solution is given are the semimajor axis, the eccentricity, the inclination of the orbit to the lunar equator, the angle of the line of nodes measured from the line joining the earth and moon in the lunar equatorial plane, the angle of periselenium (the closest approach to the moon), and finally the time of periselenium. The semimajor axis and eccentricity are both found to be constant from this solution, and the differential equations describing the remaining parameters are functions only of the inclination and line of nodes. The solutions for the latter two may be given in terms of elliptic functions of the time, and thus the behavior of every parameter may be expressed by known functions or by integrals of known functions.

Solution and Main Conclusions

Because the solution applies only to near circular orbits, the angle and time of periselenium are not important or well-defined parameters. The most interesting information can be obtained from the integrals describing the orientation of the orbit, i.e., the inclination and line of nodes, and when the altitude of the orbit is between 50 and 1000 km., these two quantities are given by

$$\sin^2 i (c \sin^2 \gamma + m) - 2 \cos i = k \quad (6)$$

$$\cos i = \frac{d \operatorname{sn}^2(\phi) + \ell}{f \operatorname{sn}^2(\phi) + g} \quad (7)$$

where γ is the line of nodes; i is the inclination; and $\operatorname{sn}(\phi)$ indicates the elliptic sine function. The quantity ϕ is a linear function of the time, and the remaining quantities in Eqs. (6) and (7) are constants depending upon the initial conditions and the system parameters, i.e., the gravitational constants, earth-moon distance, etc.

It can be shown from these expressions that $\cos(i)$ is periodic with a period almost exactly half that of the moon's revolution about the earth, and the limits of its variation can be easily calculated. For equatorial orbits, both direct and retrograde, the inclination is constant. As the inclination approaches 90° the amplitude of the variation in $\cos(i)$ increases, reaching a maximum at a value of i slightly greater than 90° , and at this point the variation in i is less than $1^\circ.5$. Because γ is measured from a rotating reference line, namely, the earth-moon line, it is a constantly decreasing quantity. However, its rate of decrease may be altered by proper choice of initial conditions to be slightly greater or less than the rate at which the earth-moon line rotates. This means that measured from an inertial reference, the line of nodes of a lunar satellite orbit may be made either to advance or regress by choice of initial conditions. But the rate of advance or regression is extremely small, amounting to less than $0^\circ.1$ per month for orbits with altitudes between 50 and 1000 km. The over-all picture which this approximate solution gives of near circular lunar satellite orbits is, then, the following: The major axis and eccentricity remain fixed while the inclination undergoes a small periodic variation and the line of nodes experiences a very small secular rate of change.

The question arises of the accuracy of this picture, and a partial answer can be found in the section on Numerical Study which follows. It will be noted from Figs. 1 through 5 that the semimajor axis of the computed solutions does remain constant on the average but that it also undergoes a periodic variation with period one half the orbital period of the satellite. The eccentricity is not constant, but from an initial value of zero it

never exceeds 0.001. Figures 3 through 5 are graphs of orbits with an initial inclination of 90° , and they corroborate the predicted motion in i . The magnitude of the oscillation is also within the limits predicted by the approximate solution. However, if Eq. (6) is solved for $\cos i$, the resulting formula predicts incorrectly the direction of change of i , that is, whether i increases or decreases from its initial value. The motion of the line of nodes is much larger in the numerical solutions than in the analytic, but it is still small, amounting to no more than 3° , and follows no obvious pattern. Therefore, the general agreement of the numerical solutions with the approximate analytic one can be said to be good, save one exception in the motion of i . And the average solution seems to have served the purpose of delineating the important general features of the motion of a lunar satellite.

NUMERICAL STUDY

Explanation of Graphs and Tables

At the end of this report are 7 tables and 12 graphs, listed as Figs. 2 through 13. Each figure has the same format, and each represents one lunar satellite orbit. Eight quantities are plotted. The first five are parameters of the orbit, and the remaining three are radius and velocity components. The parameters are:

- a the semimajor axis in kilometers
- e the eccentricity
- i_E the inclination taken with respect to the
 earth's equator
- Ω_E the angle of the line of nodes measured in
 the earth equatorial plane from the vernal
 equinox
- ω_E the angle of periselenium (closest approach)
 measured in the plane of the orbit from the
 line of nodes. Plotted only for eccentric
 orbits.

It will be noted that i_E , Ω_E , and ω_E are measured in an earth equatorial system. This is the system in which the orbits were computed, and it was chosen because it approximates an inertial frame much more closely than a lunar equatorial system. The data might still be presented in the latter form, but the motion of the moon would then introduce extraneous, purely geometrical, perturbations in the listed quantities. However, the initial conditions for each orbit are given in Table 1, which immediately precedes the graphs, in terms of the lunar frame because the differences in perturbations are more closely related to it. The radius and velocity components are listed on the graphs as r ; w , the circumferential velocity; and u , the radial velocity. Their units are kilometers and kilometers per second respectively. Finally, the time scale of the graphs requires explanation. To plot each orbit for the entire 13 days for which it was computed would be cumbersome and would obscure essential information. Therefore, each orbit is plotted during five intervals of approximately 4-1/4 hours duration, and these intervals are evenly spaced at slightly more than three days.

Tables 2 through 5 are tabulations of perturbations in the radius and orbital parameters versus the initial conditions of each orbit. As in Table 1 these initial conditions are given in the selenographic coordinate system at the initial time. The quantities listed are:

Δr	the difference between maximum and minimum radius in kilometers
Δa	the difference between maximum and minimum a in kilometers
Δa_m	the difference between maximum and minimum values of the mean value of a
e_{\max}	maximum eccentricity
Δi_E	the difference between maximum and minimum inclination
$\Delta \Omega_E$	the difference between maximum and minimum angle of the line of nodes

Because the semimajor axis varies periodically but with a near constant mean value, the variation in this mean value has been tabulated along with the parameters.

Table 2 lists eight orbits with the initial time of 9 January 1969. These are from Group 1 of the schedule of inputs, and thus evidence the effects of all the perturbing forces. Table 3 consists of four orbits with initial conditions identical to the first four from Table 2, but only the lunar perturbations were included in their computation. They are from the third group of the schedule of inputs. Tables 4 and 5 are identical to Table 2 except in initial times which are 17 December 1963 and 5 January 1960 respectively.

The remaining two tables list the position errors as a result of changes in the values of the astrodynamical constants. Table 6 gives the initial conditions of two orbits and the two values of the astronomical unit which were used in computing each orbit. The positions are given after 2 months time and the differences in kilometers computed. Table 7 lists the initial conditions of a 45° lunar orbit and the two values of each lunar principal axis which were used. The positions after one half a month are given and the differences listed.

Tables 8 through 12, Appendix C, cover the entire schedule of inputs, and their format is identical to that outlined above.

The Plan of Computation

The over-all purpose of the numerical portion of this contract has been to survey the perturbations of a wide variety of lunar satellite orbits. To perform this task adequately, many different perturbations must be considered and their relative magnitudes compared. In addition, the times at which the satellite orbits are computed must be varied since the perturbations change as the moon's orbit changes. Finally, each orbit must be computed for a considerable length of time so that the magnitude of the changes in the orbit will be sufficiently large, and this implies that a numerical integration routine must be employed which possesses an unusually high degree of accuracy.

Tables 8 through 12 contain a schedule of initial orbital parameters which was designed to meet the requirement of a wide variety of satellite orbits. The parameters are given with respect to the selenographic coordinate system, that is, the inclination is measured with respect to the plane of the lunar equator, and the line of nodes is measured in the same plane from the first principal axis of the moon. The plan of computation centers about a large group of orbits with the same initial time of 9 January 1969. This first group includes orbits with different altitudes, inclinations, and eccentricities, and all the principal perturbations were included in computing each orbit. These perturbations are due to the asphericity of the moon and the attractions of the earth, sun, and planets.

The second and third groups of orbits from the schedule are smaller, and are subgroups of the first. They have identical initial conditions and starting time, but not all the perturbations have been included in their computation. The second group includes the perturbations of the triaxial moon and the attraction of the earth but does not include the influences of the sun and planets. The third includes only the perturbations due to the moon. By examining the changes in these orbits, it is possible to compare the magnitudes of the separate perturbations.

The fourth and fifth groups have initial times of 17 December 1963 and 5 January 1960, respectively, but their initial conditions are otherwise identical to a subgroup of the first group of orbits.

Figure 1 is a schematic diagram of the positions of earth, moon, and sun at the three initial times. The symbol, \uparrow , indicates the direction of the vernal equinox; \uparrow is the ascending node of the moon's orbit in the ecliptic and the large semicircle represents the path of the moon during the computation of each satellite orbit. The moon's orbit precesses in the ecliptic with an 18-year period, and these three initial times represent three significantly different configurations during this cycle.

A further goal of this study has been the determination of position errors due to uncertainties in the astrodynamical constants. To this end the astronomical unit and the lengths of the principal axes of the moon have been varied between the limits of their probable errors and the resulting orbits compared. The initial parameters of these orbits are listed as the final group in the schedule of inputs of Appendix C.

Each orbit of the preceding groups was computed for one half of a lunar sidereal month except for those from the final group, some of which were computed for two months. In order to meet the demands of numerical accuracy which this imposes, a variation of parameters integration routine was developed for the IBM 7094 digital computer. The derivation of the equations for this routine is contained in Appendix B. The equations are applicable to all but rectilinear orbits, and the routine makes possible the computation of satellite motion for a considerable length of time with small error. The table at the end of Appendix B demonstrates this for a simple example.

The constants which have been used throughout the numerical study have been taken from Ref. 4; however, the variations in the astronomical unit and principal axes of the moon were calculated from Ref. 5. The form of the moon's potential follows closely that of Ref. 6 and the transformation equations between selenocentric and selenographic coordinates were taken from Ref. 3.

Conclusions

The numerical solutions which have been obtained under this contract show clearly that there are no ironclad formulas for predicting the perturbations of a lunar satellite. However, certain classes of orbits exhibit common features worth noting. Those which are most easily characterized are the circular and near-circular cases.

An orbit with an initial eccentricity of zero will remain near-circular for a considerable period. In no instance among the orbits computed did the eccentricity rise as high as 0.001 from an initial value of zero, and many of these orbits were calculated for more than 200 revolutions. Evidence that the eccentricity might become appreciable after a longer period of time is lacking. No secular changes in e are detectable. Thus, analytic approximations to satellite motion which depend upon assumptions of near circularity are very likely to remain valid for considerable periods of time.

The semimajor axis of low eccentricity orbits displays an interesting character. In every case it has a periodic variation with period one half that of the orbit and a mean value which is very nearly constant. This behavior is clearly evident in Fig. 2. For most cases the amplitude of the variation is considerably smaller than the variation in the radius itself, but Fig. 4 shows the opposite situation. Here, the radius experiences little change, and this points up a well-known but interesting fact. To compute orbits with very small eccentricity, a polar coordinate system can be superior to a set of parameters. For moderate and high eccentricities, however, the parameters have a clear advantage.

The changes in the orientation of a near circular orbit — the inclination and line of nodes — depend on the initial conditions. Orbits lying in the lunar equatorial plane, both direct and retrograde, are extremely stable. As the initial value of the inclination increases, however, it develops a periodic character; the orbit nodes. As predicted by the analytic solution of the Approximate Solution Section, the period is one half the lunar sidereal month, and the amplitude is largest near 90° . And, as Table 2 shows, the oscillation does not exceed $1^\circ.5$.

The direction in which the orbit nods, that is, whether the inclination increases or decreases from its initial value, appears to be governed by the initial angle of the line of nodes. In Figs. 3 and 5 the initial value of γ is 0° and the inclination increases, whereas in Fig. 4 a γ of 90° causes i_E to decrease. It should be pointed out that, though the plotted inclination is determined with respect to the earth's equator, a simple transformation shows that these observations are true in a selenographic coordinate system. And note should also be made of the fact that the periodic behavior in i_E cannot truly be inferred from these plots because the time scale is not sufficiently long. Orbits which have been computed for many months, however, verify the predicted oscillation.

Unfortunately, no such conclusions can be drawn about the line of nodes. Its changes are small in the earth equatorial system, but the direction and magnitude follow no clearly discernible pattern.

The over-all behavior of eccentric orbits is not very different from the near-circular case, but in general, the perturbations are larger. The semimajor axis exhibits the same periodic character but with a varying amplitude, and the mean value changes irregularly. The eccentricity shows no secular change, and it does not vary by more than 0.001 from its initial value. But the inclination shows less stability; near-equatorial eccentric orbits can vary as much in inclination as polar orbits. Figures 10 through 13 are graphs of eccentric orbits, and they contain a trace for an additional parameter, the angle of closest approach to the moon, which for appreciable eccentricities is well-defined.

Figures 6 through 9 and Table 3 contain data on near-circular orbits perturbed only by the moon's asphericity. It will be seen that they do not differ noticeably from the same orbits in Figs. 2 through 5 and Table 2, which were computed with all the principal perturbations. It can be concluded that for orbits with altitude less than 1000 km the principal perturbations are due to the triaxial potential of the moon.

The initial conditions for the orbits listed in Tables 4 and 5 are identical to those in Table 2 except for the starting times. The different configurations corresponding to these times are shown in the schematic of Fig. 1. It can be seen immediately from the tables that the magnitudes of the perturbations at the different times are quite comparable to one another, and it can also be shown that the character of the perturbations is essentially the same.

Tables 6 and 7 of this report list differences in position as a result of using different values of the astronomical unit and of the lengths of the principal axes of the moon. They show that by far the largest errors can be expected from uncertainty in the principal axes, and this is an inevitable result of the fact that for the orbits considered, the moon's perturbations are dominant.

RECOMMENDATIONS FOR FUTURE STUDY

The previous sections show clearly that lunar orbits with altitudes less than 1000 km are very stable. Earlier work of other authors indicates, however, that the earth's influence is a strong source of instability above 2000 km. It can be supposed that exploration of the intermediate region would produce both interesting and useful results.

REFERENCES

1. Edwards, J.W., "Introduction to Non-Linear Mechanics," Ann Arbor, Michigan, 1947.
2. Lass, Harry, The Motion of a Satellite of the Moon, JPL Technical Release No. 34-56, April 28, 1960.
3. Kalensher, B.E., Selenographic Coordinates, JPL Technical Report No. 32-41, February 1961.
4. Clarke, Victor C. Jr., Constants and Related Data used in Trajectory Calculations at the Jet Propulsion Laboratory, JPL Technical Report No. 32-273, May 1, 1962.
5. Makemson, Baker, and Westrom, Analysis and Standardization of Astrodynamic Constants, Astrodynamical Report No. 12, February 1961.
6. Baker and Makemson, Astrodynamics, Academic Press, New York, 1960.

TABLE 1
Initial Orbital Parameters for Figs. 2 through 13

Initial Time = 9 January 1969, Final Time = 23 January 1969						
Fig.	Initial Orbital Parameters in Selenographic System -					Perturbations
	a	e	i			
2	1788 km	0.0	0°0.0	0°0.0	0°0.0	Earth, Moon, Sun, and Planets "
3	1788	0.0	90°0.0	0°0.0	0°0.0	
4	1788	0.0	90°0.0	90°0.0	0°0.0	
5	2038	0.0	90°0.0	0°0.0	0°0.0	"
6	1788 km	0.0	0°0.0	0°0.0	0°0.0	Lunar Only
7	1788	0.0	90°0.0	0°0.0	0°0.0	"
8	1788	0.0	90°0.0	90°0.0	0°0.0	"
9	2038	0.0	90°0.0	0°0.0	0°0.0	"
10	2263	.2098	5°0.0	0°0.0	0°0.0	Earth, Moon, Sun, and Planets "
11	2263	.2098	90°0.0	0°0.0	0°0.0	
12	2263	.2098	175°0.0	0°0.0	0°0.0	
13	2263	.2098	90°0.0	90°0.0	0°0.0	

TABLE 2
Perturbations of Lunar Orbits at 9 January 1969

Initial Time = 9 January 1969

Final Time = 23 January 1969

Initial Orbital Elements in Selenographic System				Perturbations of the Orbit Moon, Earth, Sun, and Planets Included					
a	e	i	γ	Δr	Δa	Δa_m	e_{max}	Δi_E	$\Delta \Omega_E$
1788 km	0.0	0° 0.0	0° 0.0	1.4286 km	0.4309 km	0.0099 km	7.690×10^{-4}	0° 0.02063	0° 0.1125
1788	0.0	90° 0.0	0° 0.0	1.0486	1.2830	0.0072	5.601×10^{-4}	1° 0.168	0° 0.2097
1788	0.0	90° 0.0	90° 0.0	0.4437	1.2802	0.0125	4.444×10^{-4}	1° 0.127	0° 0.5139
2038	0.0	90° 0.0	0° 0.0	1.0616	1.1468	0.0108	4.403×10^{-4}	0° 0.7547	0° 0.07401
2263	0.2098	5° 0.0	0° 0.0	952.8952 km	0.9468	0.2269	0.2117	0° 0.09451	1° 0.658
2263	0.2098	90° 0.0	0° 0.0	948.0785	1.8068	0.2550	0.2098	0° 0.5826	0° 0.05195
2263	0.2098	175° 0.0	0° 0.0	949.9559	0.9718	0.2552	0.2107	0° 0.08894	2° 0.823
2263	0.2098	90° 0.0	90° 0.0	948.1102	1.6143	0.2678	0.2099	0° 0.3989	0° 0.1638

TABLE 3
Perturbations of Lunar Orbits Due to the Moon Only

Initial Time = 9 January 1969

Final Time = 23 January 1969

Initial Orbital Parameters in Selenographic System				Perturbations of the Orbit Lunar Perturbations Only					
a	e	i	γ	Δr	Δa	Δa_m	e_{max}	Δi_E	$\Delta \Omega_E$
1788 km	0.0	0° 0.0	0° 0.0	1.463 km	0.4193 km	0.0008	7.806×10^{-4}	0° 0.003552	0° 0.01076
1788	0.0	90° 0.0	0° 0.0	1.1623	1.264	0.0049	5.474×10^{-4}	1° 0.167	0° 0.2307
1788	0.0	90° 0.0	90° 0.0	0.5747	1.259	0.0091	4.345×10^{-4}	1° 0.116	0° 0.5117
2038	0.0	90° 0.0	0° 0.0	0.9997	1.1051	0.0038	4.177×10^{-4}	0° 0.7379	0° 0.09893

TABLE 4

Perturbations of Lunar Orbits at 17 December 1963

Initial Time = 17 December 1963

Final Time = 31 December 1963

Initial Orbital Parameters in Selenographic System				Perturbations of the Orbit Moon, Earth, Sun, and Planets Included					
a	e	i	γ	Δr	Δa	Δa_m	e_{max}	Δi_E	$\Delta \Omega_E$
1788 km	0.0	0° 0	0° 0	1.4468 km	0.4280 km	0.00285 km	7.548×10^{-4}	0° 02637	0° 03230
1788	0.0	90° 0	0° 0	1.0324	1.280	0.00395	5.575×10^{-4}	1° 138	0° 5880
1788	0.0	90° 0	90° 0	0.5150	1.285	0.00455	4.471×10^{-4}	1° 191	0° 2049
2038	0.0	90° 0	0° 0	0.9376	1.133	0.00175	4.332×10^{-4}	0° 7244	0° 3618
2263	0.2098	5° 0	0° 0	948.3	1.014	0.2796	0.2107	0° 8547	0° 2130
2263	0.2098	90° 0	0° 0	946.2	1.746	0.2730	0.2099	0° 5656	0° 2763
2263	0.2098	175° 0	0° 0	944.7	1.005	0.3081	0.2108	0° 5047	0° 3379
2263	0.2098	90° 0	90° 0	944.0	1.630	0.2900	0.2101	0° 5981	0° 06598

TABLE 5

Perturbations of Lunar Orbits at 5 January 1960

Initial Time = 5 January 1960

Final Time = 19 January 1960

Initial Orbital Parameters in Selenographic System				Perturbations of the Orbit Moon, Earth, Sun, and Planets Included					
a	e	i	γ	Δr	Δa	Δa_m	e_{max}	Δi_E	$\Delta \Omega_E$
1788 km	0.0	0° 0	0° 0	1.467 km	0.4429 km	0.0082 km	7.891×10^{-4}	0° 005192	0° 01361
1788	0.0	90° 0	0° 0	0.9847	1.289	0.00415	5.472×10^{-4}	1° 171	0° 2109
1788	0.0	90° 0	90° 0	0.5495	1.259	0.01815	4.795×10^{-4}	1° 097	0° 5476
2038	0.0	90° 0	0° 0	0.8570	1.145	0.0140	4.274×10^{-4}	0° 7412	0° 07565
2263	0.2098	5° 0	0° 0	950.2	0.8932	0.2467	0.2111	0° 08102	2° 238
2263	0.2098	90° 0	0° 0	948.1	1.822	0.2669	0.2099	0° 5623	0° 04206
2263	0.2098	175° 0	0° 0	942.1	0.8938	0.2455	0.2099	0° 05748	1° 579
2263	0.2098	90° 0	90° 0	944.1	1.604	0.2716	0.2101	0° 5173	0° 2200

TABLE 6

Variation in Position Due to Variation in the Astronomical Unit

Initial Orbital Parameters in Selenographic System					
a	e	i	γ	Initial Time	Final Time
2738 km	0.0	0° 0	0° 0	9 January 1969	7 March 1969
Astronomical Unit	Coordinates of the Final Position			Position Error	
1.4973503x10 ⁸ km	-2735.8793 km	- 77.340972 km	-8.37345 km	0.083599 km	
1.4946297x10 ⁸	-2735.8793	- 77.263487	-8.37345		

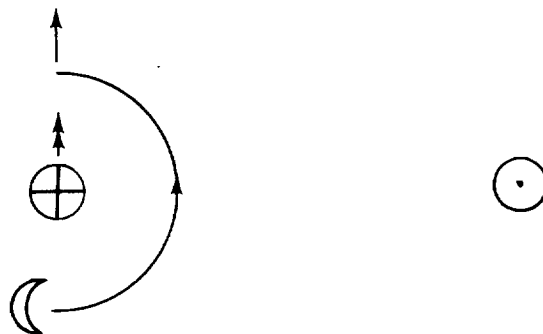
Initial Orbital Parameters in Selenographic System					
a	e	i	γ	Initial Time	Final Time
2738 km	0.0	90° 0	0° 0	9 January 1969	7 March 1969
Astronomical Unit	Coordinates of the Final Position			Position Error	
1.4973503x10 ⁸ km	-2308.1829 km	-778.44363 km	1248.5809 km	51.622669 km	
1.4946297x10 ⁸	-2334.9129	-764.63768	1206.6309		

TABLE 7

Variation in Position Due to Variation in the Principal Axes of the Moon

Initial Orbital Parameters in Selenographic System						
a	e	i	γ	Initial Time		Final Time
1788 km	0.0	45° 0	0° 0	9 January 1969		23 January 1969
Principal Axes			Coordinates of Final Position			Position Error
1738.64 km	1738.21 km	1737.49 km	1656.642 km	123.39423 km	661.20554 km	140.89688 km
1738.50	1738.21	1737.49	1704.2964	87.833989	533.46964	
1738.57	1738.28	1737.49	1686.0255	90.365741	588.26944	37.8301285
1738.57	1738.14	1737.49	1676.9499	121.12685	608.33200	
1738.57	1738.21	1737.56	1700.0171	103.64213	544.16960	114.1094070
1738.57	1738.21	1737.42	1661.5376	108.31794	651.49351	

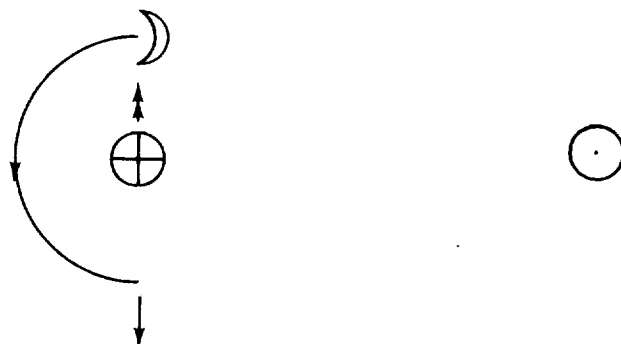
TIME = 9 JANUARY 1969



TIME = 17 DECEMBER 1963



TIME = 5 JANUARY 1960



EARTH



INDICATES DIRECTION OF
MOON'S ASCENDING NODE.
IN THE ECLIPTIC.



MOON



INDICATES DIRECTION OF
VERNAL EQUINOX.



SUN



INDICATES MOON'S PATH
DURING ONE HALF MONTH
FOLLOWING THE EPOCH.

Fig. 1 Schematic of Earth, Moon, and Sun Configurations at Three Epochs

Research Dept.
RE-170
November 1963

Initial Orbital Parameters

a	e	i	γ
1788 km	0	0°	0°

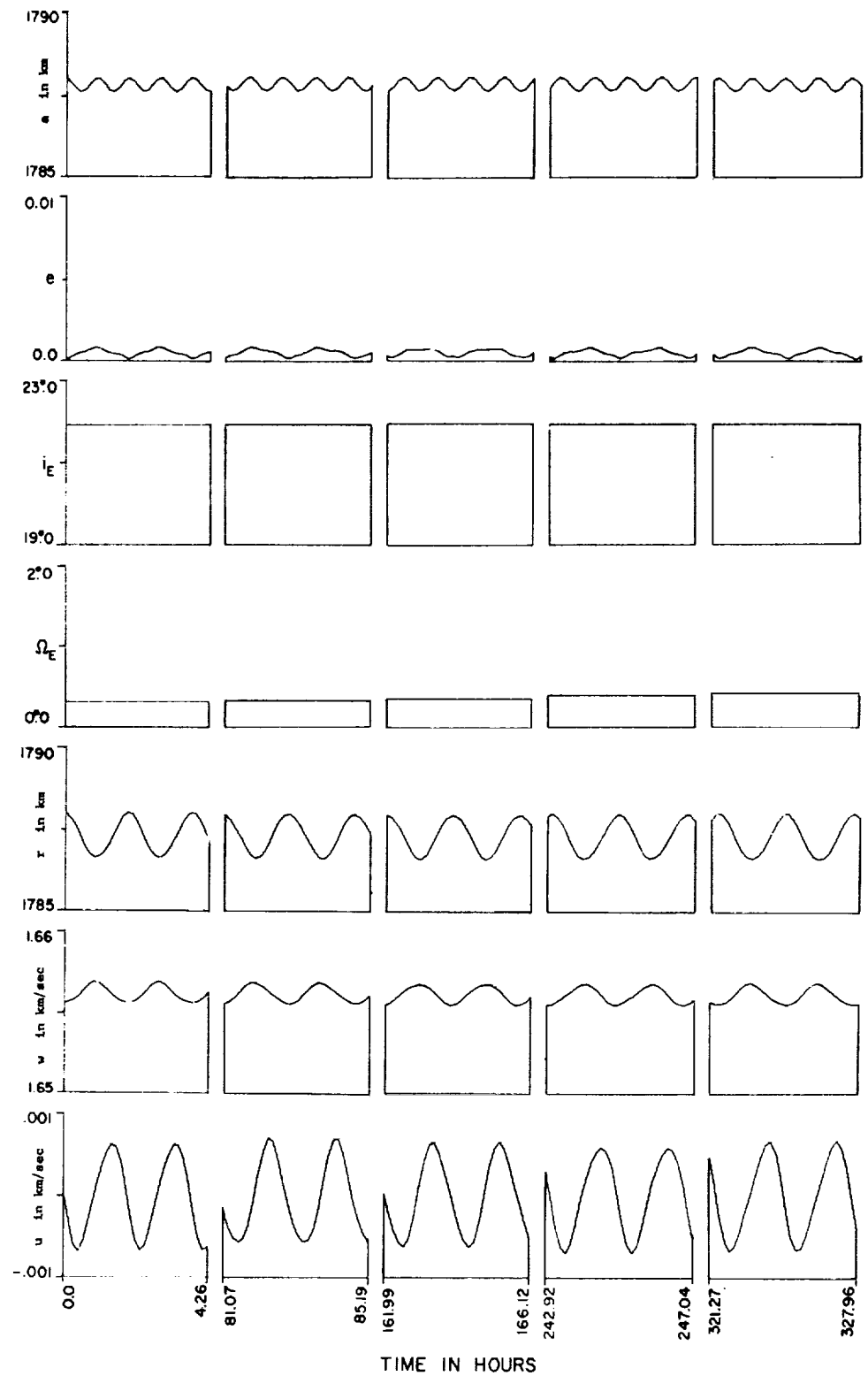


Fig. 2 Lunar Satellite Orbit Perturbed by Earth, Moon, Sun, and Planets at 9 January 1969

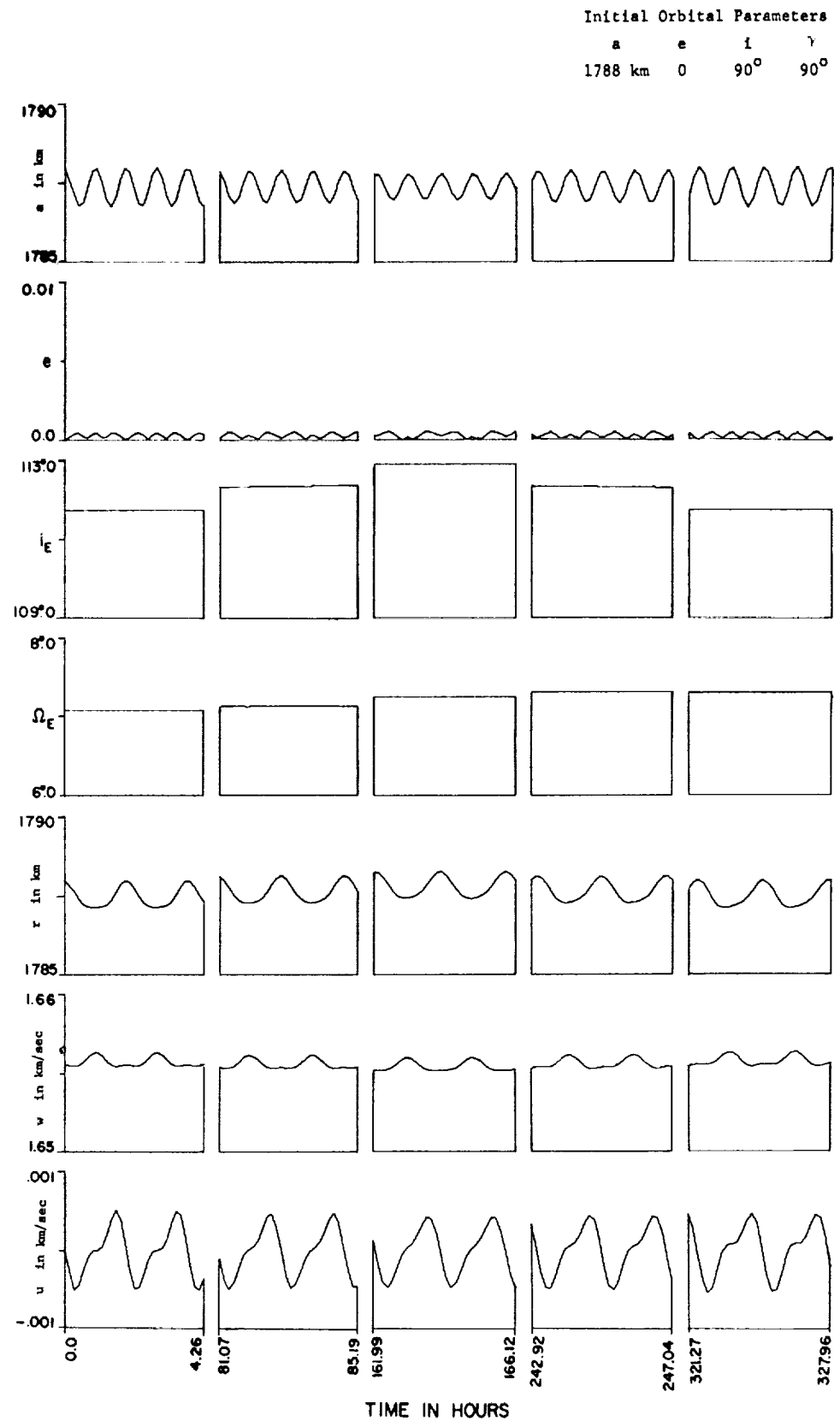


Fig. 3 Lunar Satellite Orbit Perturbed by Earth, Moon, Sun, and Planets at 9 January 1969

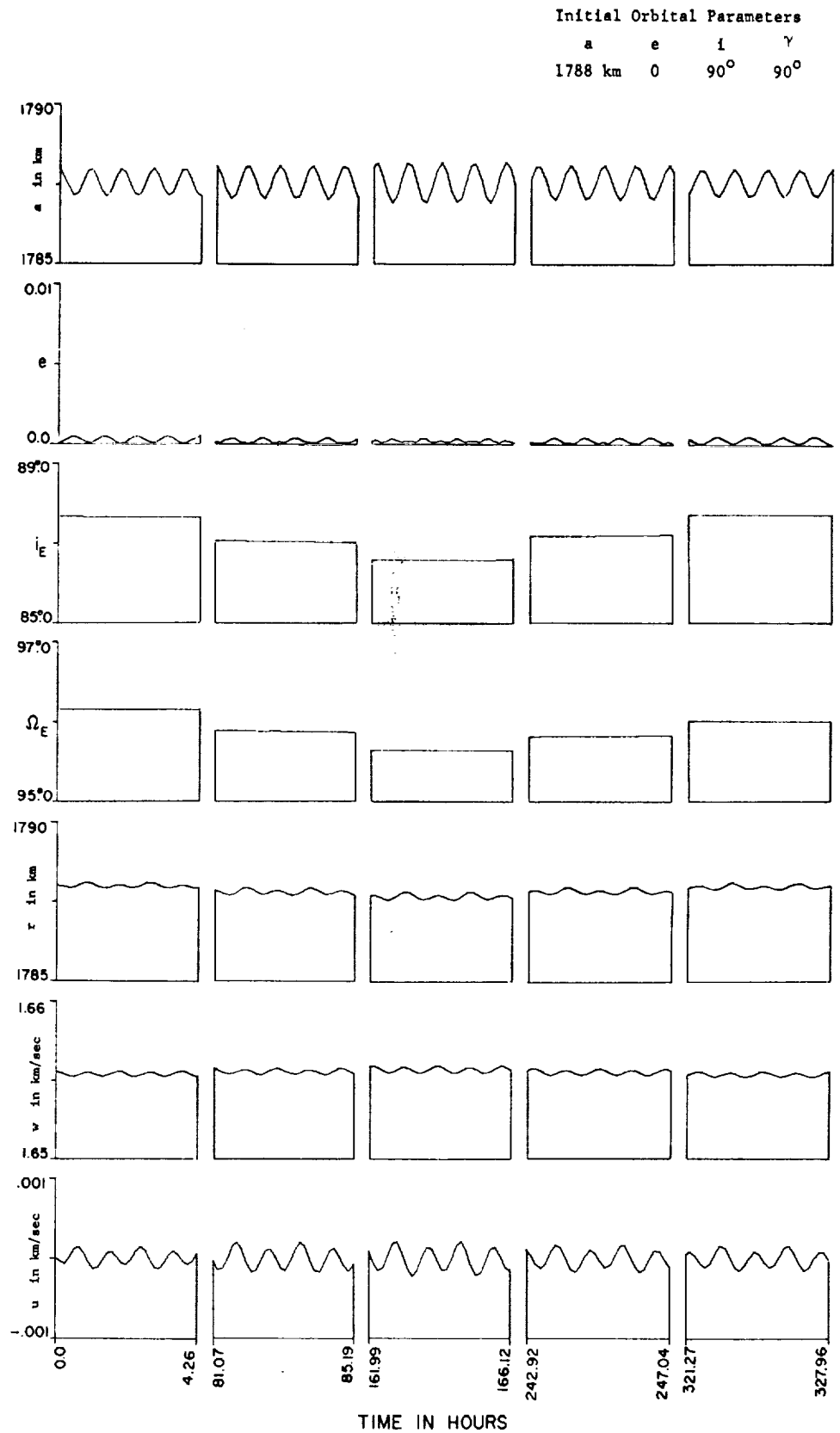


Fig. 4 Lunar Satellite Orbit Perturbed by Earth, Moon, Sun, and Planets at 9 January 1969

Initial Orbital Parameters

a	e	i	γ
2038 km	0	90°	0°

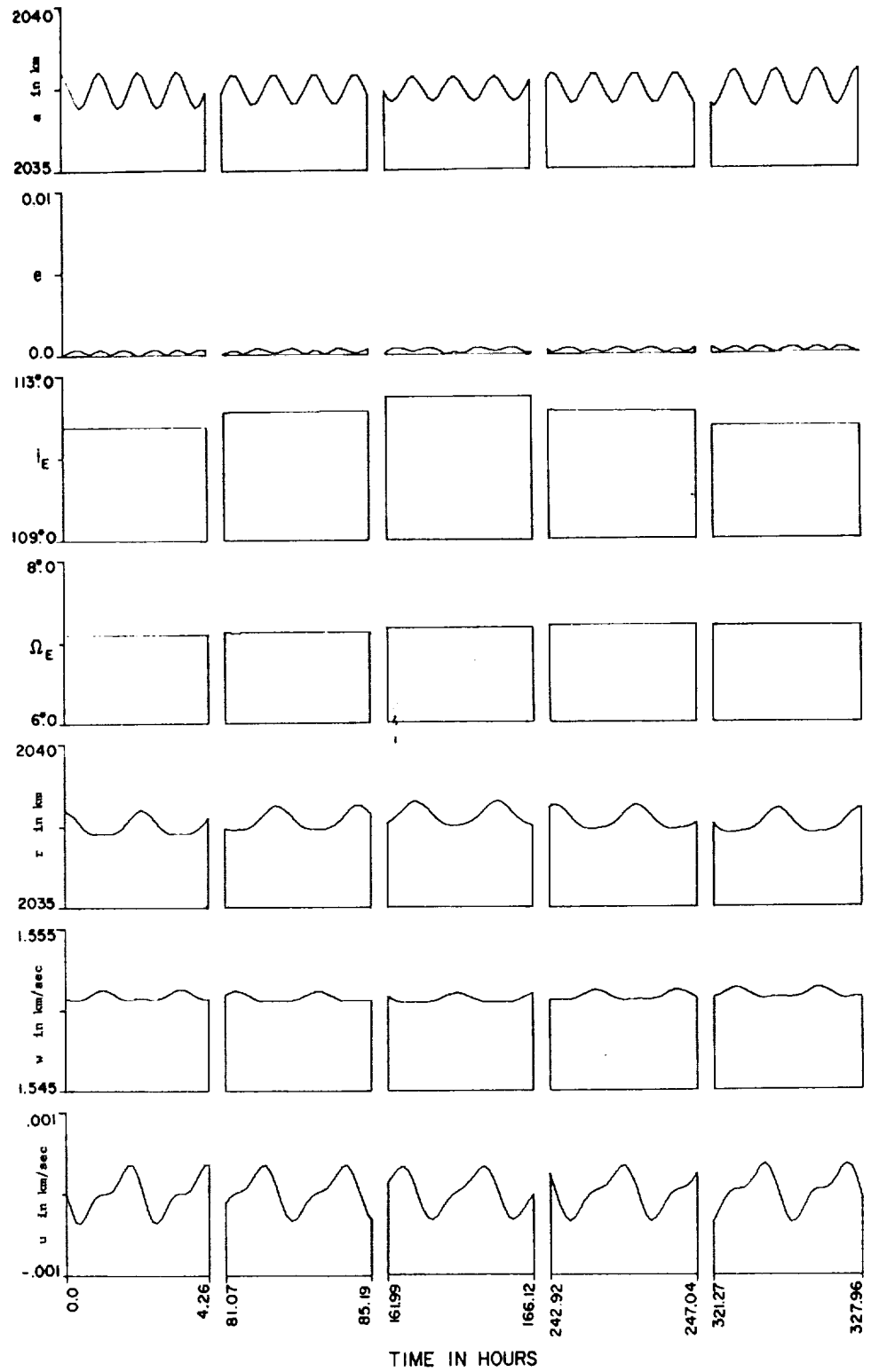


Fig. 5 Lunar Satellite Orbit Perturbed by Earth, Moon, Sun, and Planets at 9 January 1969

Initial Orbital Parameters

a	e	i	γ
1788 km	0	0°	0°

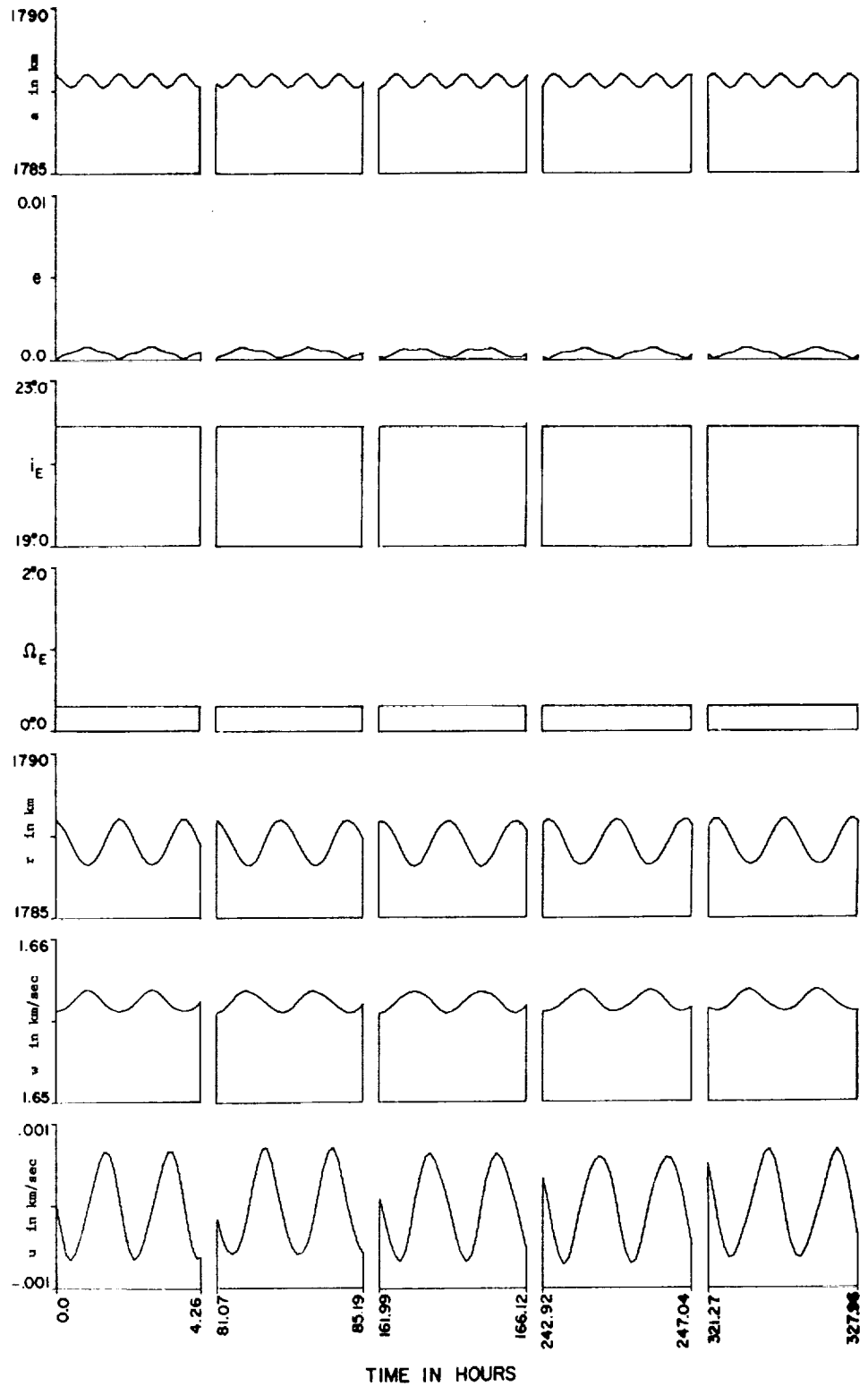


Fig. 6 Lunar Satellite Orbit Perturbed Only by the Triaxial Moon

Initial Orbital Parameters

a	e	i	γ
1788 km	0	90°	0°

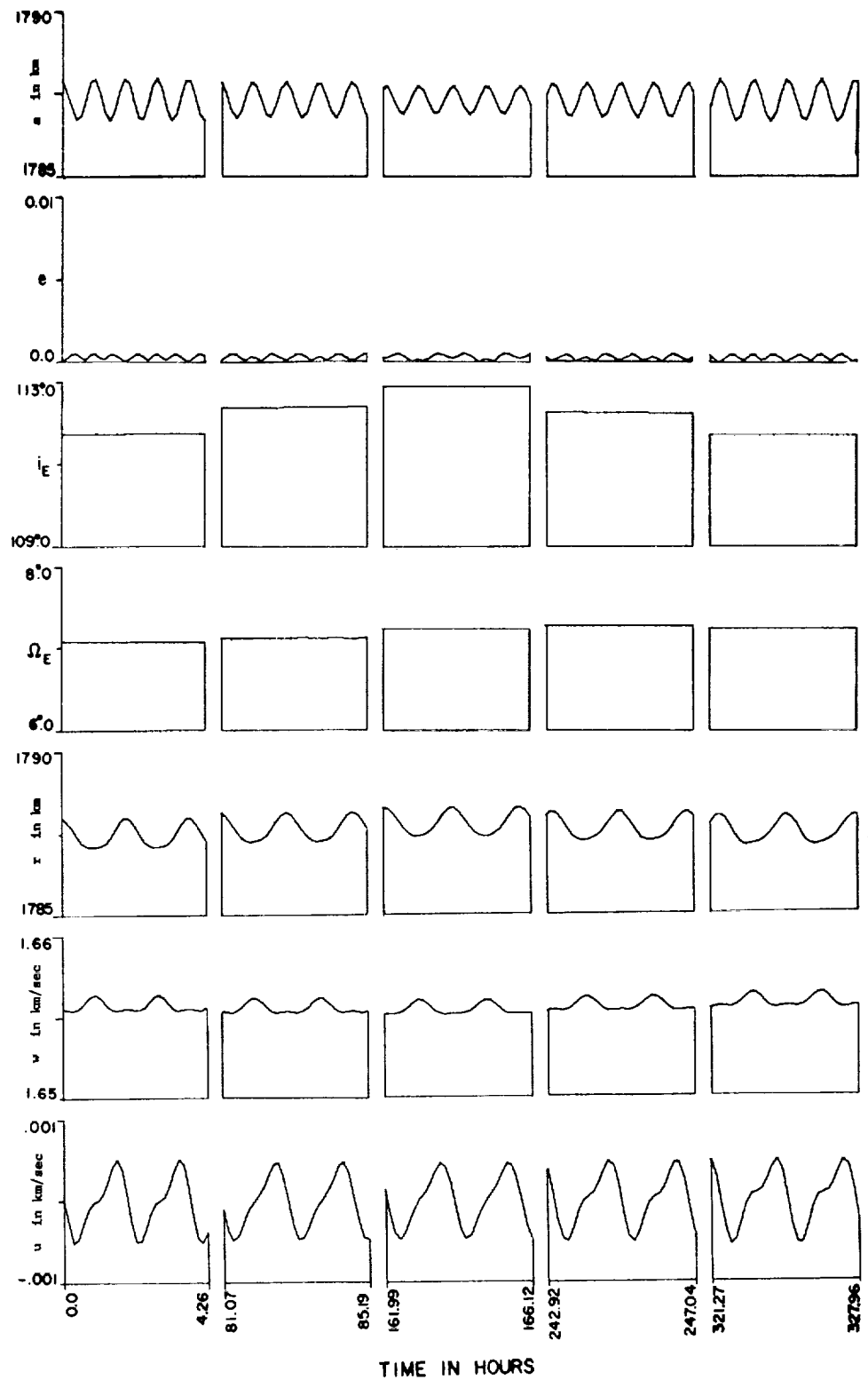


Fig. 7 Lunar Satellite Orbit Perturbed Only by the Triaxial Moon

Initial Orbital Parameters

a	e	i	γ
1788 km	0	90°	90°

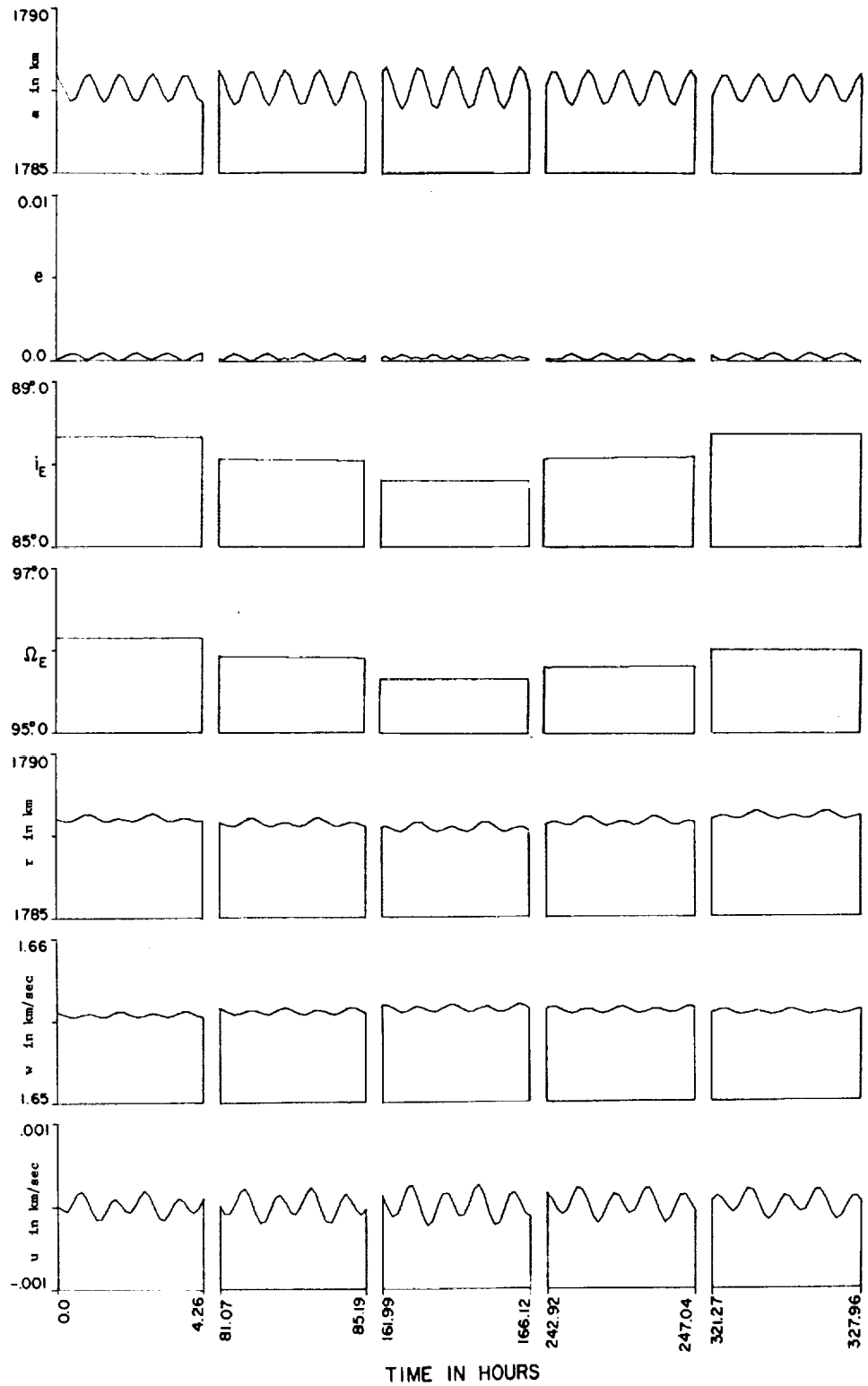


Fig. 8 Lunar Satellite Orbit Perturbed Only by the Triaxial Moon

Initial Orbital Parameters

a	e	i	γ
2038 km	0	90°	0°

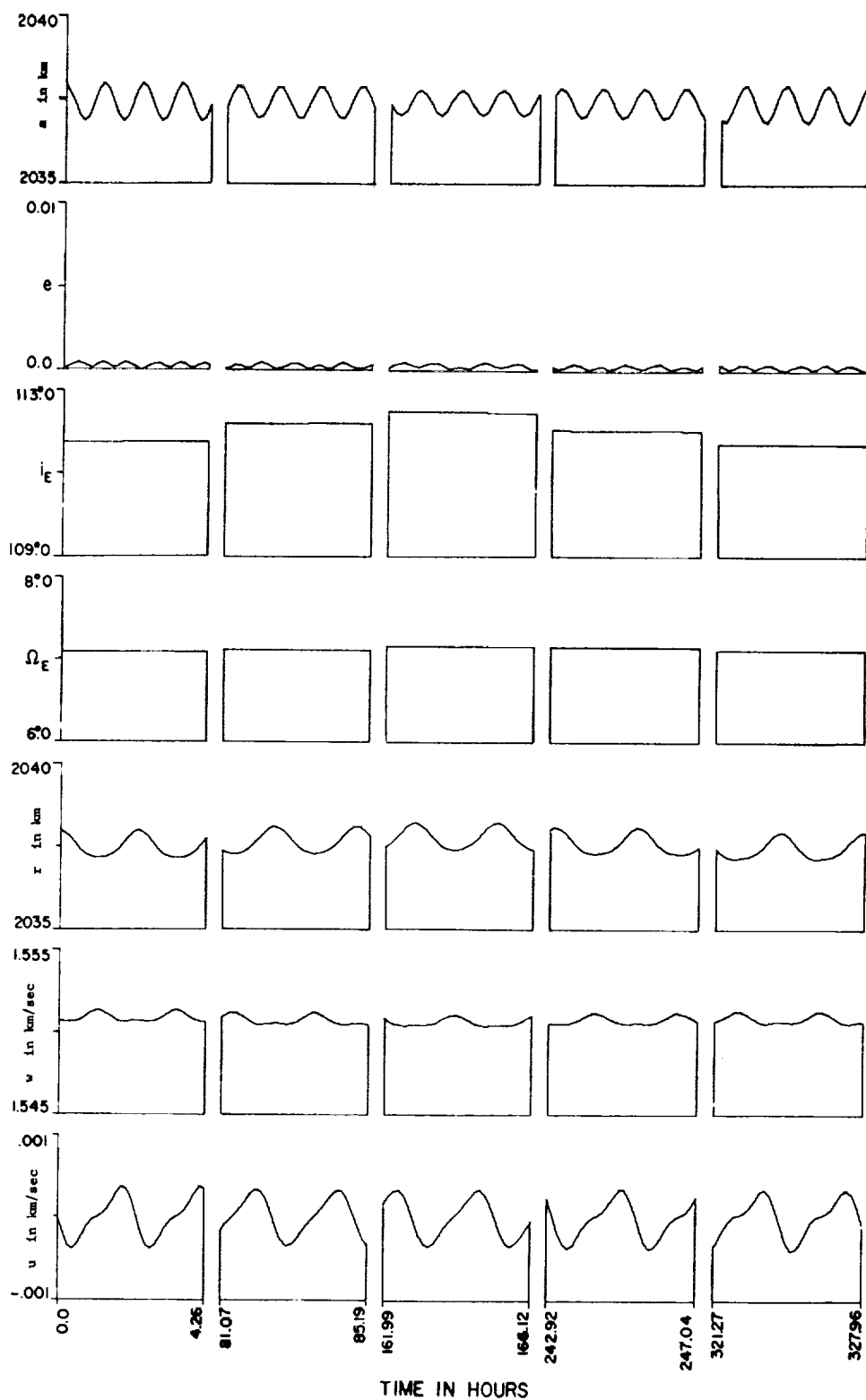


Fig. 9 Lunar Satellite Orbit Perturbed Only by the Triaxial Moon

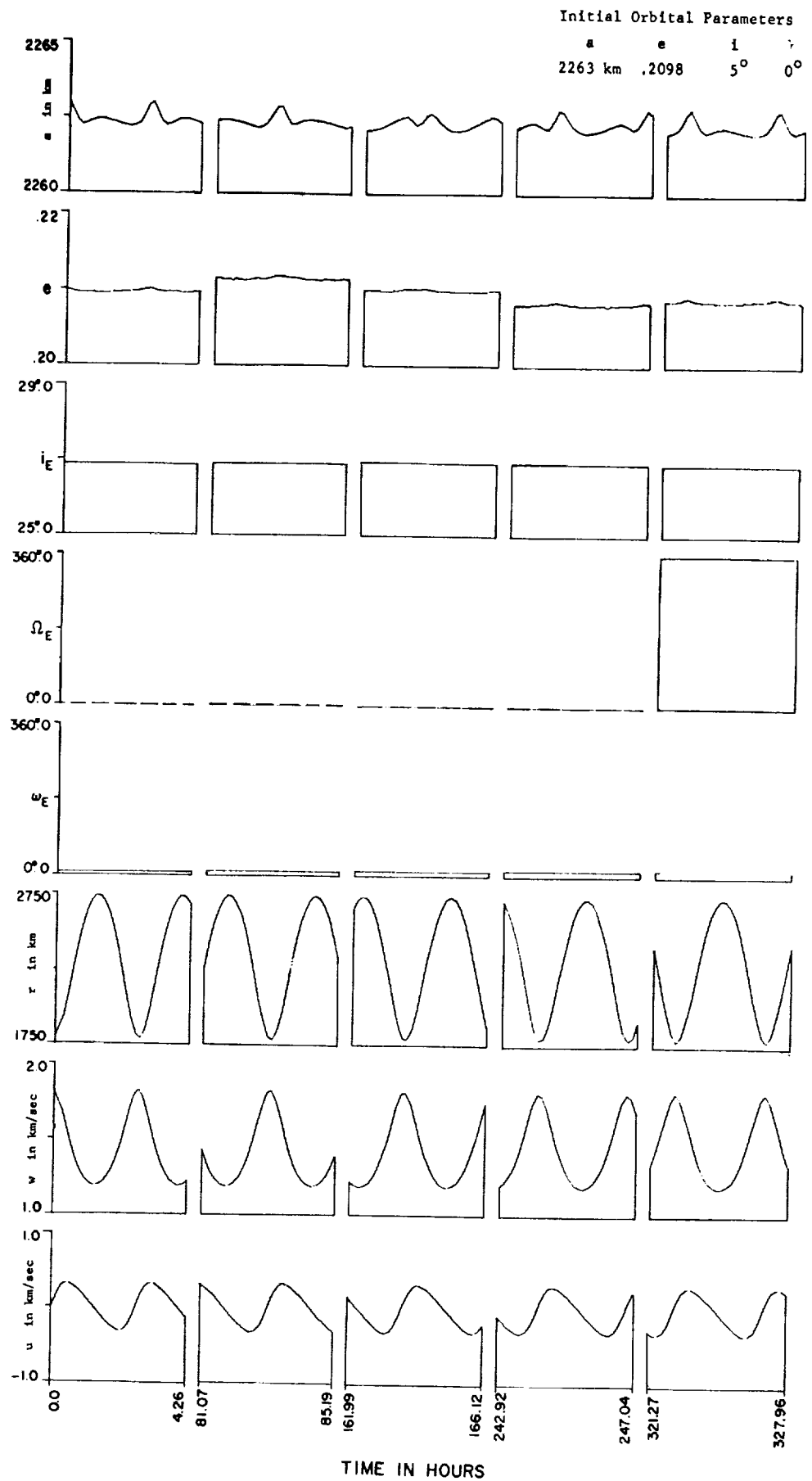


Fig. 10 Eccentric Lunar Satellite Orbit Perturbed by the Earth, Moon, Sun, and Planets at 9 January 1969

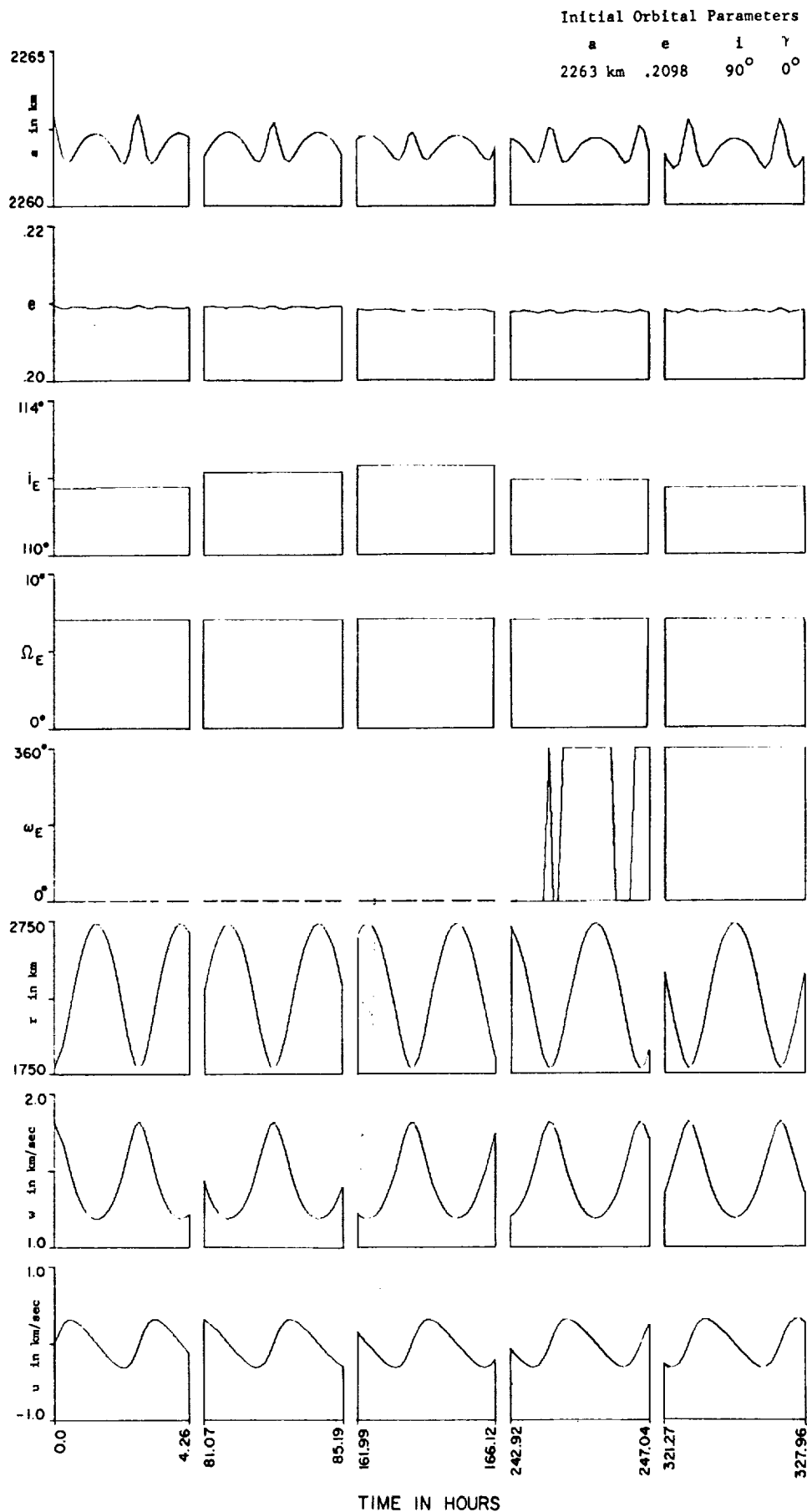


Fig. 11 Eccentric Lunar Satellite Orbit Perturbed by the Earth, Moon, Sun, and Planets at 9 January 1969

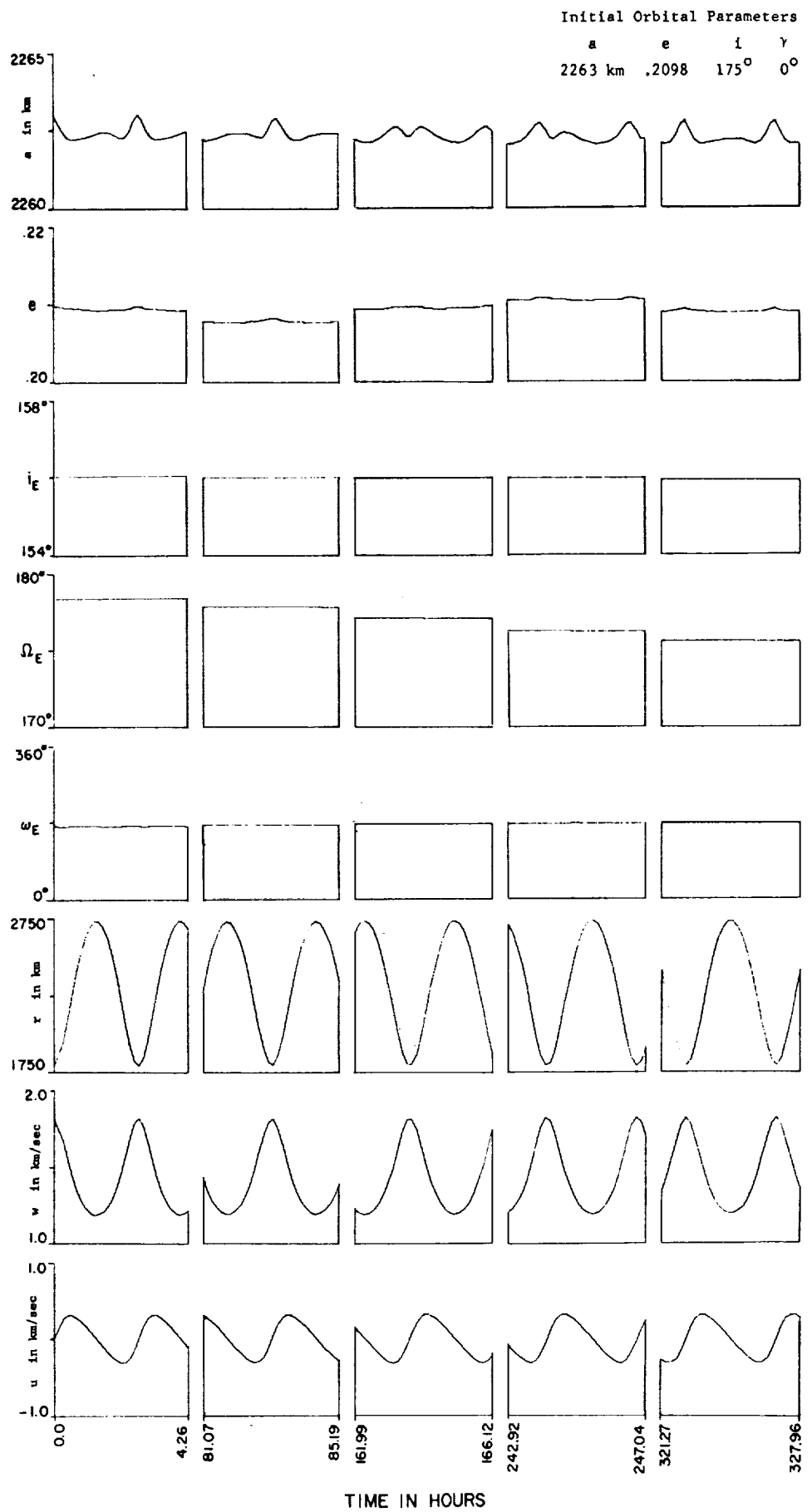


Fig. 12 Eccentric Lunar Satellite Orbit Perturbed by the Earth, Moon, Sun, and Planets at 9 January 1969

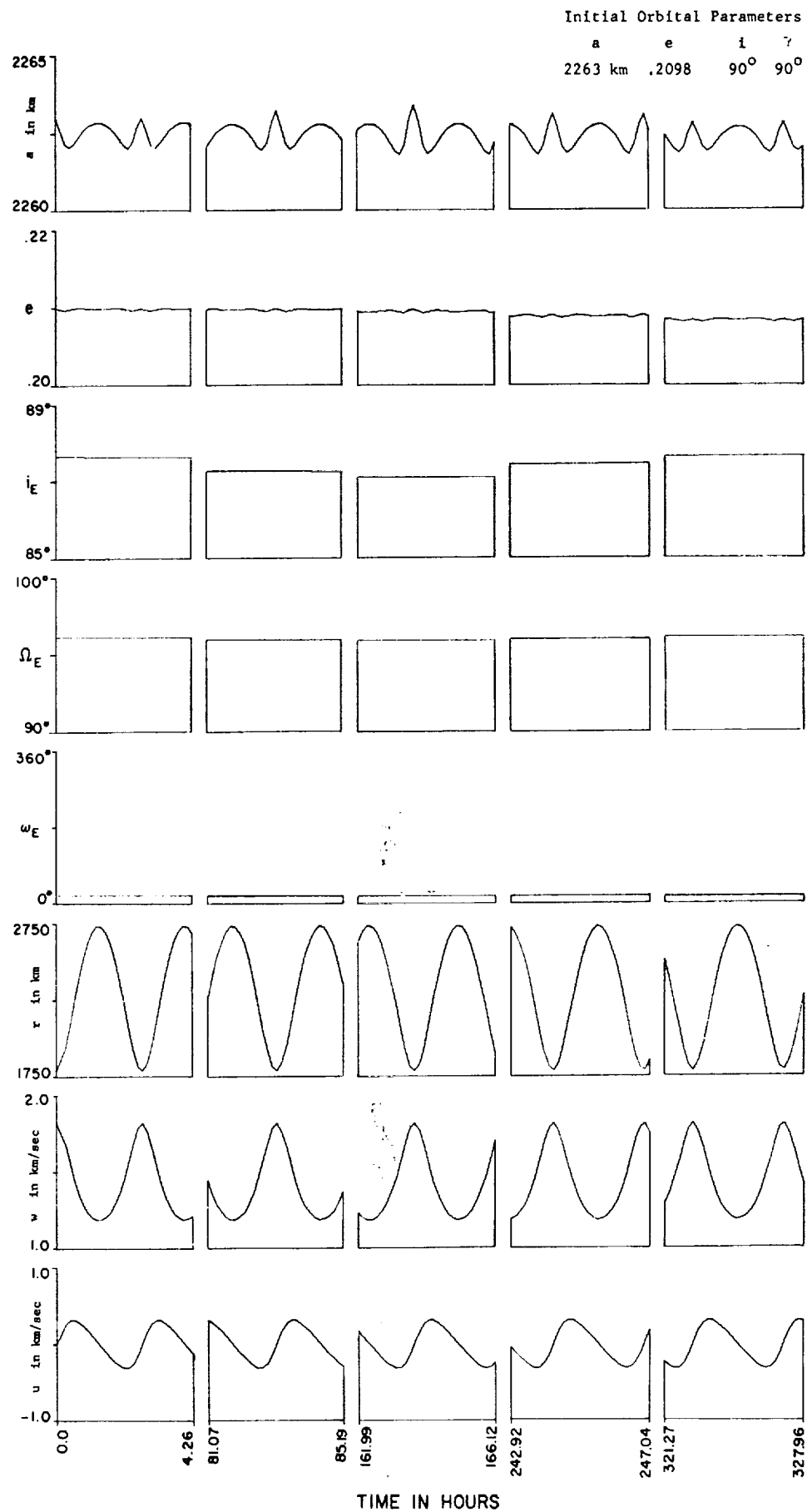


Fig. 13 Eccentric Lunar Satellite Orbit Perturbed by the Earth, Moon, Sun, and Planets at 9 January 1969

APPENDIX A
THE AVERAGE MOTION
OF A
LUNAR SATELLITE

Let R be the disturbing function for a lunar satellite perturbed by a point mass earth and sun and by a triaxial moon. R may be written in a moon-centered coordinate system as

$$\begin{aligned}
 R = & k_E \left[\left(r_E^2 + r^2 - 2r_E r \cos S_1 \right)^{-1/2} - r_E^{-2} r \cos S_1 \right] + \\
 & + k_S \left[\left(r_S^2 + r^2 - 2r_S r \cos S_2 \right)^{-1/2} - r_S^{-2} r \cos S_2 \right] + \\
 & + k_m \left[\left(\Lambda/3r^3 \right) \sum_{j=1}^3 \left(3a_j^2 - 1 \right) b_j^2 \right].
 \end{aligned} \tag{1}$$

Expanding R in terms of r/r_E and r/r_S and keeping second order terms, we find

$$\begin{aligned}
 R \approx & k_E \left[r_E^{-1} + r_E^{-1} \left(3 \cos^2 S_1 - 1 \right) \left(r^2/2r_E^2 \right) \right] + \\
 & + k_S \left[r_S^{-1} + r_S^{-1} \left(3 \cos^2 S_2 - 1 \right) \left(r^2/2r_S^2 \right) \right] + \\
 & + k_m \left[\left(\Lambda/3r^3 \right) \sum_{j=1}^3 \left(3a_j^2 - 1 \right) b_j^2 \right].
 \end{aligned} \tag{2}$$

We may drop constant terms since R is a potential function and call the result \tilde{R} . Averaging \tilde{R} over a cycle of the lunar satellite, assuming the earth and moon fixed, we have

$$\begin{aligned}
 \langle \tilde{R} \rangle = & (k_E r_E^{-3}) (a^2/4) \left\{ 3(E_E^2 + D_E^2) - 2 + 3e^2(4D_E^2 - E_E^2 - 1) \right\} + \\
 & + (k_S r_S^{-3}) (a^2/4) \left\{ 3(E_S^2 + D_S^2) - 2 + 3e^2(4D_S^2 - E_S^2 - 1) \right\} + \\
 & + \left(k_m^{5/2} \Lambda / 2a^{3/2} h^3 \right) \left\{ b_1^2 (\cos^2 \gamma + \cos^2 i \sin^2 \gamma) + \right. \\
 & \quad + b_2^2 (\sin^2 \gamma + \cos^2 i \cos^2 \gamma) + \\
 & \quad \left. + b_3^2 (\sin^2 i) - (2/3) B_4 \right\}, \tag{3}
 \end{aligned}$$

where

$$E_p = \cos \omega \cos(\phi_p - \Omega) + \cos i \sin \omega \sin(\phi_p - \Omega) \tag{4}$$

$p = E, S$

$$D_p = -\sin \omega \cos(\phi_p - \Omega) + \cos i \cos \omega \sin(\phi_p - \Omega)$$

If the orbital element Ω is replaced by the new element $\gamma = \Omega - \phi_E$, the elements α_1, β_1 with $\beta_3 = -\gamma$ will be canonical if the term $\delta_E \alpha_3$ is added to the disturbing function. Letting $\bar{R} = \langle \tilde{R} \rangle + \delta_E \alpha_3$ the canonical system is written

$$\frac{d\alpha_i}{dt} = - \frac{\partial \bar{R}}{\partial \beta_i} , \quad \frac{d\beta_i}{dt} = \frac{\partial \bar{R}}{\partial \alpha_i} , \quad i = 1, 2, 3 . \quad (5)$$

The only restriction placed on the satellite orbit by the development of these equations is that the ratios r/r_E and r/r_S be small. However, a solution to this system is not available, and additional approximations must be made.

An explicit time dependence occurs in the terms E_S and D_S in the angle $\Omega - \phi_S$. To eliminate it, an average of \bar{R} is taken with respect to the time over the period $2\pi/(\delta_E - \delta_S)$. Finally, the presence of e^2 in Eq. (3) introduces h and h_z in a complicated fashion, therefore we assume e^2 to be very small and disregard all terms containing it as a factor. With these approximations the potential function becomes

$$\begin{aligned} R_p = & (k_E r_E^{-3})(a^2/4) \left\{ 3(\cos^2 \gamma + \cos^2 i \sin^2 \gamma) - 2 \right\} + \\ & + (k_S r_S^{-3})(a^2/4) \left\{ (3/2)(1 + \cos^2 i) - 2 \right\} + \\ & + \left(k_m^{5/2} \Lambda / 2a^{3/2} h^3 \right) \left\{ b_1^2 (\cos^2 \gamma + \cos^2 i \sin^2 \gamma) + \right. \\ & \quad + b_2^2 (\sin^2 \gamma + \cos^2 i \cos^2 \gamma) + \\ & \quad + b_3^2 \sin^2 i - (2/3) B_4 \left. \right\} + \\ & + \delta_E h \cos i . \end{aligned} \quad (6)$$

The associated differential equations are

$$\frac{da}{dt} = 0 \quad (7)$$

$$\frac{dh}{dt} = 0 \quad (8)$$

$$\frac{di}{dt} = \frac{1}{h} \left\{ 6(k_E r_E^{-3})(a^2/4) + (b_1^2 - b_2^2) \left(k_m^2 \Lambda / a^{3/2} h^3 \right) \right\} \sin i \cos \gamma \sin \gamma \quad (9)$$

$$\begin{aligned} \frac{d(nT)}{dt} = & (k_E r_E^{-3}) \left(\sqrt{a^3/k_m} \right) \left\{ 3(\cos^2 \gamma + \cos^2 i \sin^2 \gamma) - 2 \right\} + \\ & + (k_S r_S^{-3}) \left(\sqrt{a^3/k_m} \right) \left\{ (3/2)(1 + \cos^2 i) - 2 \right\} + \\ & - (k_m^2 \Lambda) (3/2 a^2 h^3) \left\{ b_1^2 (\cos^2 \gamma + \cos^2 i \sin^2 \gamma) + \right. \quad (10) \\ & + b_2^2 (\sin^2 \gamma + \cos^2 i \cos^2 \gamma) + \\ & \left. + b_3^2 \sin^2 i - (2/3) B_4 \right\} \end{aligned}$$

$$\begin{aligned}
\frac{d\omega}{dt} = & (k_E r_E^{-3})(3a^2/2h) \cos^2 i \sin^2 \gamma + \\
& + (k_S r_S^{-3})(3a^2/4h) \cos^2 i + \\
& + (k_m^{5/2} \Lambda) (3/2 a^{3/2} h^4) \left\{ b_1^2 (\cos^2 \gamma + \cos^2 i \sin^2 \gamma) + \right. \\
& \quad + b_2^2 (\sin^2 \gamma + \cos^2 i \cos^2 \gamma) + \\
& \quad + b_3^2 \sin^2 i - (2/3) B_4 \left. \right\} + \\
& + (k_m^{5/2} \Lambda / a^{3/2} h^4) \left\{ (b_1^2 \sin^2 \gamma + b_2^2 \cos^2 \gamma - b_3^2) \cos^2 i \right\}
\end{aligned} \tag{11}$$

$$\begin{aligned}
\frac{d\gamma}{dt} = & - \frac{1}{h} \left\{ 6(k_E r_E^{-3})(a^2/4) + (b_1^2 - b_2^2)(k_m^{5/2} \Lambda / a^{3/2} h^3) \right\} \cos i \sin^2 \gamma + \\
& - \frac{1}{h} \left\{ 3(k_S r_S^{-3})(a^2/4) + (b_2^2 - b_3^2)(k_m^{5/2} \Lambda / a^{3/2} h^3) \right\} \cos i + \\
& - \delta_E .
\end{aligned} \tag{12}$$

Because a and h are constants, the equations for i and γ can be solved separately. In more compact notation, letting $d\tau = \delta_E dt$, they have the form

$$\frac{di}{d\tau} = c \sin i \cos \gamma \sin \gamma \quad (13)$$

$$\frac{d\gamma}{d\tau} = -1 - \cos i (c \sin^2 \gamma + m) ,$$

and these have the first integral

$$\sin^2 i (c \sin^2 \gamma + m) - 2 \cos i = K , \quad \text{a constant} . \quad (14)$$

An additional integral may be given in terms of elliptic functions. But the representation is different depending on the magnitudes of c and m , and these vary with the orbital altitude. However, for orbits with altitude less than 1000 km and greater than 50 km, the second integral is given without exception as

$$\cos i = \frac{d \operatorname{sn}^2(\mu(\tau_0 - \tau) + \lambda, k) + \ell}{f \operatorname{sn}^2(\mu(\tau_0 - \tau) + \lambda, k) + g} . \quad (15)$$

If we define auxiliary quantities r_1, \dots, r_4 by

$$\begin{aligned} r_1 &= \left(-1 + \sqrt{1 + (c+m)(c+m-K)} \right) / (c+m) \\ r_2 &= \left(-1 + \sqrt{1 + m(m-K)} \right) / m \\ r_3 &= \left(-1 - \sqrt{1 + (c+m)(c+m-K)} \right) / (c+m) \\ r_4 &= \left(-1 - \sqrt{1 + m(m-K)} \right) / m \end{aligned} \quad (16)$$

then

$$d = r_3(r_1 - r_2)$$

$$e = -r_2(r_1 - r_3)$$

$$f = (r_1 - r_2)$$

$$g = - (r_1 - r_3)$$

(17)

$$k^2 = (r_1 - r_2)(r_3 - r_4) / (r_1 - r_3)(r_2 - r_4)$$

$$\mu = \sqrt[4]{\left\{1 + (c + m)(c + m - K)\right\} \left\{1 + m(m - K)\right\}}$$

$$\lambda = \text{a constant of integration}$$

The quantities r_i are the roots of the fourth order polynomial from which the elliptic functions arise, and their order and magnitudes determine the form of the second integral. For the cases we are considering, $r_1 \geq r_2 > r_3 > r_4$ and $r_1 \geq \cos i \geq r_2$.

Physical Interpretations

The first integral is a useful relation for exploring the behavior of $\cos i$. If we solve for $\cos i$, we find

$$\cos i = \left(-1 + \sqrt{1 + (c \sin^2 \gamma + m)(c \sin^2 \gamma + m - K)} \right) / (c \sin^2 \gamma + m) \quad (18)$$

where the choice of a plus sign before the radical is required by the values of c and m . In its original form the integral shows that for equatorial orbits $K = \pm 2$. In Eq. (18) these values of K show $\cos i = +1$ independently of γ , and thus the inclination of an equatorial orbit, either direct or retrograde, does not change. This could have been conjectured from the physical model adopted. Another quantity of interest is $(\cos i_{\max} - \cos i_{\min})$ for a given orbit. With the range of values for c and m with which we are concerned

$$\cos i_{\max} - \cos i_{\min} = \frac{c+m\sqrt{1+(c+m)(c+m-K)} - (c+m)\sqrt{1+m(m-K)}}{m(c+m)} \quad (19)$$

And the maximum of this function occurs when $K = c + 2m$ giving

$$\max\{\cos i_{\max} - \cos i_{\min}\} = c\left(\frac{1 - \sqrt{1 - m(c+m)}}{m(c+m)}\right) \quad (20)$$

If we expand the square root and take the first two terms, this maximum can be shown less than .023. Therefore the inclination does not vary more than 12° regardless of the initial values of i and γ .

The second integral is most useful for determining the period of the motion of the inclination. Since the period of the elliptic sine depends on k , we must calculate it as well

as μ . Two different polar orbits will be considered. For the first, $\sin^2 \gamma_0 = 1$, so $K = c + m$. The quantity $\mu = .99988$ for a 1000 km altitude circular orbit with these initial conditions, and $k^2 = .08538$ giving a period of $(2\pi + .1412)$ for $\sin \psi$ and $\frac{1}{2}(2\pi + .1412)$ for $\sin^2 \psi$. The period in seconds for $\cos i$ is then 1.19276×10^6 sec, and this is 1.0226 times the half period of the earth's motion about the moon. In the second case we choose $\sin^2 \gamma_0 = 0$ so $K = m$. The quantity μ becomes 1.0706 for the same altitude orbit and $k^2 = .063717$, giving a period for $\sin^2 \psi$ of $\frac{1}{2}(2\pi + .1008)$ and a period for $\cos i$ which is .949 times the half period of the earth's motion.

An inspection of Eq. (18) shows that the period of $\sin \gamma$ should be twice that of $\cos i$ since only $\sin^2 \gamma$ appears. Thus the initial conditions of a satellite orbit can be so chosen that the period of γ is either slightly greater or less than that of the earth's revolution about the moon and the period of i will be one half that. In inertial coordinates this means that the line of nodes of the orbit can be made either to advance or regress on the average.

APPENDIX B

A VARIATION-OF-PARAMETERS SCHEME

FOR LUNAR ORBITS

Derivation

Many different variation-of-parameters schemes exist for describing the motion of a vehicle in a perturbed central force field. Some have difficulty with small divisors when the eccentricity is small, and many are inapplicable to near-parabolic and hyperbolic motion. The following note traces the derivation of one variation-of-parameters scheme which has singularities only for rectilinear orbits and zero inclination, and has the advantage of simplicity and ease of computation. Since orbits with zero inclination are often the most interesting, it should be noted that a simple change of coordinate system, though not an elegant device, will eliminate this singularity for any particular orbit; and it will be shown that the form of the differential equations is invariant under this coordinate change.

The parameters chosen are the semilatus rectum of the osculating orbit, the products of the eccentricity with the sine and cosine of the angle of pericenter, and the three Euler angles describing the orientation of the osculating orbit and the position of the vehicle in the orbit. It will be observed that this last angle is not a constant for unperturbed motion. But in using it we avoid solving Kepler's equation or an equation like it; and in practice the differential equation for this angle has proven to be well-behaved.

Our development begins with the Newtonian equations in Cartesian coordinates:

$$\frac{d^2\vec{x}}{dt^2} = -\frac{k\vec{x}}{r^3} + \vec{F} \quad (1)$$

where $r = |\vec{x}|$ and \vec{F} is the perturbing acceleration. We define three mutually perpendicular unit vectors by the following relations:

$$\vec{a} = \vec{x}/r$$

$$\vec{c} = \left(\vec{x} \cdot \frac{d\vec{x}}{dt} \right) / \left| \left(\vec{x} \cdot \frac{d\vec{x}}{dt} \right) \right| \quad (2)$$

$$\vec{b} = \vec{c} \cdot \vec{a} ,$$

and express \vec{x} and $\frac{d\vec{x}}{dt}$ as

$$\vec{x} = r\vec{a} \quad (3)$$

$$\frac{d\vec{x}}{dt} = u\vec{a} + w\vec{b}$$

The vectors \vec{a} , \vec{b} , and \vec{c} are, of course, unit vectors in the radial, circumferential, and normal directions; and they are solely functions of the three Euler angles whose derivatives we are seeking.

Differentiating Eqs. (3) and taking $\vec{F} = f\vec{a} + g\vec{b} + h\vec{c}$, we have

$$\frac{d\vec{x}}{dt} = \frac{dr}{dt} \vec{a} + r \frac{d\vec{a}}{dt} = u\vec{a} + w\vec{b} \quad (4)$$

$$\frac{d^2\vec{x}}{dt^2} = \frac{du}{dt} \vec{a} + u \frac{d\vec{a}}{dt} + \frac{dw}{dt} \vec{b} + w \frac{d\vec{b}}{dt} = \left(-\frac{k}{r^2} + f \right) \vec{a} + g\vec{b} + h\vec{c} \quad (5)$$

By taking appropriate dot products of Eqs. (4) and (5), the time derivatives of r , u , and w can be found.

$$\frac{d\vec{x}}{dt} \cdot \vec{a} = \frac{dr}{dt} = u$$

$$\frac{d^2\vec{x}}{dt^2} \cdot \vec{a} = \frac{du}{dt} + w \left(\frac{d\vec{b}}{dt} \cdot \vec{a} \right) = -\frac{k}{r^2} + f \quad (6)$$

$$\frac{d^2\vec{x}}{dt^2} \cdot \vec{b} = u \left(\frac{d\vec{a}}{dt} \cdot \vec{b} \right) + \frac{dw}{dt} = g$$

The quantity $\frac{d\vec{b}}{dt} \cdot \vec{a}$ is obtained from:

$$\begin{aligned}\frac{d\vec{x}}{dt} \cdot \vec{b} &= r \left(\frac{d\vec{a}}{dt} \cdot \vec{b} \right) = w \\ \frac{d\vec{a}}{dt} \cdot \vec{b} &= - \frac{d\vec{b}}{dt} \cdot \vec{a}\end{aligned}\tag{7}$$

Rewriting Eqs. (6) we have:

$$\begin{aligned}\frac{dr}{dt} &= u \\ \frac{du}{dt} &= - \frac{k}{r^2} + \frac{w^2}{r} + f \\ \frac{dw}{dt} &= - \frac{uw}{r} + g\end{aligned}\tag{8}$$

In terms of the angles defined in Fig. B1, the vectors \vec{a} , \vec{b} , \vec{c} can be written:

$$\begin{aligned}\vec{a} &= (\cos \theta \cos \Omega - \sin \theta \cos i \sin \Omega, \cos \theta \sin \Omega \\ &\quad + \sin \theta \cos i \cos \Omega, \sin \theta \sin i) \\ \vec{b} &= (- \sin \theta \cos \Omega - \cos \theta \cos i \sin \Omega, \\ &\quad - \sin \theta \sin \Omega + \cos \theta \cos i \cos \Omega, \cos \theta \sin i) \\ \vec{c} &= (\sin i \sin \Omega, - \sin i \cos \Omega, \cos i) ;\end{aligned}\tag{9}$$

and the time derivatives of \vec{a} and \vec{b} are simply:

$$\begin{aligned}\frac{d\vec{a}}{dt} &= \vec{b} \left(\frac{d\theta}{dt} + \cos i \frac{d\Omega}{dt} \right) + \vec{c} \left(\sin \theta \frac{di}{dt} - \cos \theta \sin i \frac{d\Omega}{dt} \right) \\ \frac{d\vec{b}}{dt} &= \vec{a} \left(- \frac{d\theta}{dt} - \cos i \frac{d\Omega}{dt} \right) + \vec{c} \left(\cos \theta \frac{di}{dt} + \sin \theta \sin i \frac{d\Omega}{dt} \right).\end{aligned}\tag{10}$$

Using Eqs. (10), additional dot products of Eqs. (4) and (5) with the unit vectors, Eqs. (2), yield equations for the time derivatives of θ , i , and Ω .

$$\begin{aligned}
 \frac{d\vec{x}}{dt} \cdot \vec{b} &= r \left(\frac{d\vec{a}}{dt} \cdot \vec{b} \right) = w \\
 &= r \left(\frac{d\theta}{dt} + \cos i \frac{d\Omega}{dt} \right) \\
 \frac{d^2\vec{x}}{dt^2} \cdot \vec{c} &= w \left(\frac{d\vec{b}}{dt} \cdot \vec{c} \right) = h \\
 &= w \left(\cos \theta \frac{di}{dt} + \sin \theta \sin i \frac{d\Omega}{dt} \right) \\
 \frac{d\vec{x}}{dt} \cdot \vec{c} &= r \left(\frac{d\vec{a}}{dt} \cdot \vec{c} \right) = 0 \\
 &= r \left(\sin \theta \frac{di}{dt} - \cos \theta \sin i \frac{d\Omega}{dt} \right)
 \end{aligned} \tag{11}$$

The equations may be solved for the indicated derivatives whenever $\sin i \neq 0$. Thus the time variations of θ , i , and Ω have been found at least implicitly.

The remaining three parameters whose equations we are seeking are known as functions of r , u , w , and θ .

$$\begin{aligned}
 p &= r^2 w^2 / k \\
 q &= \{ (rw^2/k) - 1 \} \cos \theta + \{ rwu/k \} \sin \theta \\
 s &= \{ (rw^2/k) - 1 \} \sin \theta - \{ rwu/k \} \cos \theta
 \end{aligned} \tag{12}$$

Differentiating Eqs. (12) and substituting on the right from Eqs. (8) and (11), we may express the time derivatives of p , q , and s as functions of r , u , w , and the three Euler angles. Writing r , u , and w as functions of p , q , and s will then complete the derivation of the differential equations for our set of parameters. However, it seems easier computationally and also more meaningful physically to leave the equations as functions of r , u , and w and compute the latter quantities separately. This computation is simple to perform.

$$\begin{aligned} r &= p/(1 + q \cos \theta + s \sin \theta) \\ u &= \sqrt{k/p} (q \sin \theta - s \cos \theta) \\ w &= \sqrt{k/p} (1 + q \cos \theta + s \sin \theta) \end{aligned} \quad (13)$$

In these terms then the differential equations are:

$$\begin{aligned} \frac{dp}{dt} &= 2(r^2 w/k) g \\ \frac{dq}{dt} &= [(ru/k)g + (rw/k)f + \{(rw/k) - (1/w)\} \{h \sin \theta \cos i / \sin i\}] \sin \theta \\ &\quad + [2(rw/k)g - (ru/k)(h \sin \theta \cos i / \sin i)] \cos \theta \\ \frac{ds}{dt} &= [2(rw/k)g - (ru/k)(h \sin \theta \cos i / \sin i)] \sin \theta \\ &\quad - [(ru/k)g + (rw/k)f + \{(rw/k) - (1/w)\} \{h \sin \theta \cos i / \sin i\}] x \cos \theta \\ \frac{d\theta}{dt} &= (w/r) - (h \sin \theta \cos i / w \sin i) \\ \frac{di}{dt} &= (h \cos \theta / w) \\ \frac{d\Omega}{dt} &= (h \sin \theta / w \sin i) \end{aligned} \quad (14)$$

Coordinate Change for Low Inclinations

When i is close to 0° or 180° , division by $\sin i$ reduces the accuracy with which these equations can be computed; and exactly at 0° and 180° the equations are no longer valid. To avoid this difficulty, we redefine \vec{a} , \vec{b} , \vec{c} in terms of three different angles. This is accomplished simply by choosing a new coordinate system in our original equation for \vec{x} , Eq. (1). The new coordinate system is obtained by a 90° clockwise rotation about the x -axis of Fig. B1. Defining angles θ' , Ω' , and i' completely analogously in the new system to the definitions of θ , Ω , and i in the old, Fig. B2, it is apparent that the formal derivation of the equations follows exactly as before; but now $|i'| \geq |90^\circ - i|$.

In the context of a numerical integration routine, a coordinate change is not desirable, because it requires re-initializing the program. However, it should be pointed out that this need not occur frequently since Eqs. (14) are applicable without appreciable loss of accuracy to an approximate range of values of i from 6° to 174° .

Early Applications

The equations described above have been programmed in two dimensions, i.e., without the terms involving i and Ω ; and trajectories have been integrated employing the logarithmic spiral as a check solution. Identical trajectories have been integrated employing Eqs. (1) directly and also by the use of another variation-of-parameters scheme based on the initial conditions as parameters. Comparison of the results indicates that the program utilizing Eqs. (14) is both quicker and more accurate than either of the other two in this application and will follow the exact solution for many revolutions. Table B1 lists the results of the three programs applied to three different logarithmic spirals.

Proposed Application

Because of the success in two dimensions, the equations in three dimensions, Eqs. (14), are being programmed, and it is intended to apply them to lunar orbits. The potential of the moon will have the form:

$$\Phi = \frac{Gm}{R} + \frac{G}{2R^3}(A + B + C - 3I) \quad (15)$$

where A, B, and C are the principal moments of inertia of the lunar ellipsoid and I is the moment of inertia about \vec{R} , the vector from the moon's center to the point of space in question. The moments of inertia will be calculated assuming the moon increases slightly in density toward the center in concentric ellipsoidal shells, following a formula proposed by Jeffreys (Ref. 1); and the effects of the earth, sun, and major planets will be included. Throughout, the standardized astrodynamic constants suggested by Baker, et al. (Ref. 2) will be used.

Two additional features of the program are that it will calculate geocentric orbits and cislunar trajectories. For these applications, the earth's potential includes terms for oblateness and the pear shape. It is hoped that this program will yield information on the relative stability of lunar orbits of varying radius and angle of inclination, and that it will prove useful as a general purpose integration routine for trajectories in earth-moon space.

References

1. Jeffreys, H., Mon. Not. Roy. Astronomical Soc., Vol. 117, pp. 475-477, 1957.
2. Baker, et al., Journal of the Astronautical Sciences, Vol. VIII, No. 1, Spring 1961.

TABLE B1

Results of the Three Programs Applied to Three Different Logarithmic Spirals

Program	Cartesian Coordinates	Variation of Parameters (Initial Conditions)	Variation of Parameters (p, q, s, θ)
Initial Radius	6.8781449×10^3 km	6.8781449×10^3 km	6.8781449×10^3 km
Eccentricity*	.004777	.004777	.004777
Final Time	1.794048×10^6 sec	1.7896×10^6 sec	1.788928×10^6 sec
Final Radius	4.22085×10^4 km	4.223036×10^4 km	4.2181687×10^4 km
True Radius	4.2257×10^4 km	4.219181576×10^4 km	4.21819484×10^4 km
% Error of Radius	.115%	.0914%	.00062%
Number of Revolutions	60	60	60
Number of Inte- gration Intervals	3560	5400	587
Approximate Machine Time	.6 min	5.4 min	.2 min
Initial Radius	6.8781449×10^3 km	6.8781449×10^3 km	6.8781449×10^3 km
Eccentricity*	0.20	0.20	0.20
Final Time	4.8552336×10^9 sec	5.0720803×10^9 sec	5.133825×10^9 sec
Final Radius	9.9488194×10^7 km	9.757424×10^7 km	9.816419×10^7 km
True Radius	9.4565866×10^7 km	9.7361008×10^7 km	9.8149559×10^7 km
% Error of Radius	5.2%	.219%	.0149%
Number of Inte- gration Intervals	3072	720	340
Initial Radius	6.8781449×10^3 km	6.8781449×10^3 km	6.8781449×10^3 km
Eccentricity	0.50	0.50	0.50
Final Time	1.623468×10^9 sec	1.9687052×10^9 sec	2.0300418×10^9 sec
Final Radius	9.1022364×10^7 km	9.5314883×10^7 km	9.7394317×10^7 km
True Radius	8.3917045×10^7 km	9.5427773×10^7 km	9.7399705×10^7 km
% Error of Radius	8.47%	.118%	.005531%
Number of Inte- gration Intervals	2060	280	160

*The logarithmic spiral has a constant eccentricity; and the initial conditions of a logarithmic trajectory are completely determined by the eccentricity and the initial radius, assuming the initial angle is zero.

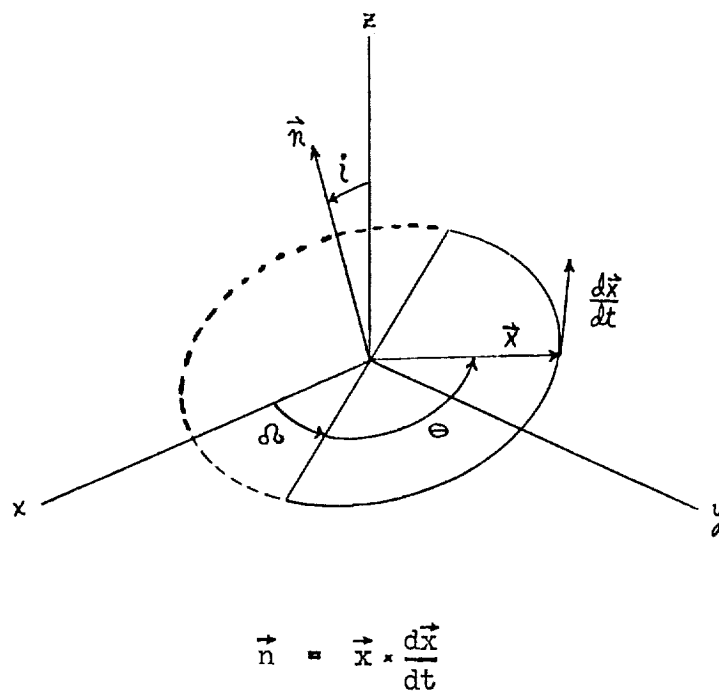


Fig. B1 Orbital Elements for High Inclinations

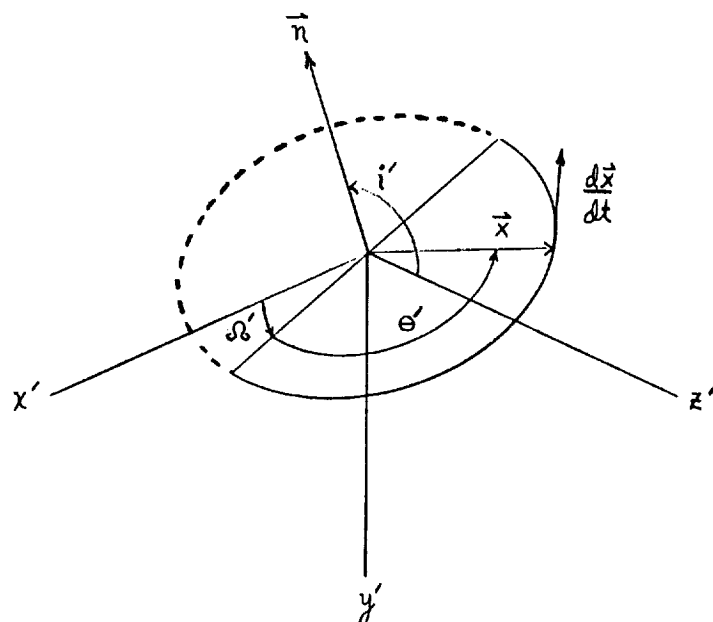


Fig. B2 Orbital Elements for Low Inclinations

APPENDIX C

CATALOG OF NUMERICAL RESULTS

TABLE 8
Schedule of Inputs

Inputs for Orbits with Initial Time = 9 January 1969					
Perturbing	Initial Orbital Elements in Selenographic System				
Bodies	a	e	i	γ	ω
Moon, Earth, Sun, and Planets	1788 km	0.0	0°	0°	0°
	2038				
	2738				
	1788		45		
	2038				
	1788		90		
	2038			90	
	2738				
	1788		135		
	1788		180		
	1788		45		
	1788		90		
	1788		135		
	1813	0.014	5	0	0
			10		
			170		
			175		
			5		
			175		
	2263	0.2098	5	0	0
			90		
			175		
			5		
			90		
			5		
			5		
			90		
Moon and Earth	1788	0.0	0	0	0
	1788		90		
	2038		90		
	1788		90		
Moon	1788	0.0	0	0	0
	1788		90		
	2038		90		
	1788		90		
	2263	0.2098	5	0	
	2263		90		

TABLE 8 (Cont'd)
Schedule of Inputs

Inputs for Orbits with Initial Time = 17 December 1963						
Perturbing	Initial Orbital Elements in Selenographic System					
Bodies	a	e	i	γ	ω	
Moon,	1788 km	0.0	0°	0°	0°	
	1788		90			
	2038		90			
Earth,	1788	0.2098	90	90		
	2263		5	0		
Sun, and	2263		90			
	2263		175			
Planets	2263		90	90		

Inputs for Orbits with Initial Time = 5 January 1960						
Perturbing	Initial Orbital Elements in Selenographic System					
Bodies	a	e	i	γ	ω	
Moon,	1788 km	0.0	0°	0°	0°	
	1788		90			
	2038		90			
Earth,	1788	0.2098	90	90		
	2263		5	0		
Sun, and	2263		90			
	2263		175			
Planets	2263		90	90		

TABLE 9

Perturbations of Lunar Orbits at 9 January 1969
Circular Orbits Perturbed by the Moon, Earth, Sun, and Planets

Initial Orbital Elements in Selenographic System					Perturbations of the Orbit					
a	e	i	γ	ω	ΔT	Δa	Δa_m	e_{max}	Δi_E	$\Delta \Omega_E$
1788 km	0	0°	0°	0°	1.4286 km	0.4309 km	0.0099 km	7.690×10^{-4}	0°.02063	0°.1125
2038					1.2637	0.3812	0.0067	5.948×10^{-4}	0°.02372	0°.1353
2738					1.1641	0.4178	0.0414	3.8707×10^{-4}	0°.03466	0°.2075
1788	45°				1.2520	0.8454	0.0062	6.2581×10^{-4}	1°.0023	10°.2688
2038					1.1061	0.7520	0.0067	4.9297×10^{-4}	0°.6525	6°.5733
1788	90°				1.0486	1.2830	0.0072	5.601×10^{-4}	1°.168	0°.2097
2038					1.0616	1.1468	0.0108	4.403×10^{-4}	0°.7547	0°.07401
2738					1.0587	0.9577	0.0128	3.1346×10^{-4}	0°.2881	0°.08036
1788	135°				1.2572	0.8530	0.0051	6.3867×10^{-4}	1°.415	22°.2998
1788	180°				1.4403	0.4293	0.0056	7.7335×10^{-4}	0°.01089	0°.1160
1788	45°	90°	0		0.4882	0.8397	0.0091	4.1320×10^{-4}	4°.5727	10°.7644
1788	90°	90°			0.4437	1.2802	0.0125	4.4444×10^{-4}	1°.127	0°.5139
1788	135°	90°			0.4298	0.8535	0.0082	3.7765×10^{-4}	4°.2001	10°.4521

TABLE 10

Perturbations of Lunar Orbits at 9 January 1969
Eccentric Orbits Perturbed by the Moon, Earth, Sun, and Planets

Initial Orbital Elements in Selenographic Systems					Perturbations of the Orbit					
a	e	i	γ	ω	ΔT	Δa	Δa_m	e_{max}	Δi_E	$\Delta \Omega_E$
1813 km	0.014	5°	0°	0°	48.8486 km	0.4469 km	0.0152 km	0.01385	0°.1734	3°.3976
		10°			48.8523	0.4587	0.0157	0.01384	0°.3220	5°.8085
		170°			48.6803	0.4630	0.0163	0.01378	0°.5157	12°.4526
		175°			48.6656	0.4529	0.0165	0.01378	0°.2543	4°.9934
		5°	90°		49.6258	0.4457	0.0150	0.01402	1°.4963	0°.9228
		175°	90°		50.1452	0.4434	0.0100	0.01419	1°.4964	0°.9230
2263 km	0.2098	5°	0°	0°	952.8952 km	0.9468 km	0.2269 km	0.2117	0°.09451	1°.658
		90°			948.0785	1.8068	0.2550	0.2098	0°.5826	0°.05195
		175°			949.9559	0.9718	0.2552	0.2107	0°.08894	2°.823
		5°	90		953.9693	0.9061	0.2304	0.2114	0°.8222	0°.2685
		90°	90		948.1102	1.6143	0.2678	0.2099	0°.3989	0°.1638
		5°	0	90	953.0346	0.8825	0.2097	0.2116	0°.0919	1°.8733
		5°	90	90	952.1121	0.9016	0.1895	0.2120	0°.8380	0°.2776

TABLE 11

Perturbations of Lunar Orbits at 9 January 1969
Circular Orbits Perturbed by the Moon and Earth

Initial Orbital Elements in Selenographic System					Perturbations of the Orbit					
a	e	i	γ	ω	ΔT	Δa	Δa_m	e_{max}	Δi_E	$\Delta \Omega_E$
1788 km	0	0°	0°	0°	1.4662 km	0.4308 km	0.0098 km	7.7076×10^{-4}	0° 02083	0° 1131
1788	0	90	0	0	1.1874	1.2829	0.0036	5.5818×10^{-4}	1° 1831	0° 2109
2038	0	90	0	0	1.0693	1.1468	0.0056	4.4027×10^{-4}	0° 7557	0° 07601
1788	0	90	90	0	0.5321	1.2798	0.0072	4.4426×10^{-4}	1° 1279	0° 5150

TABLE 12

Perturbations of Lunar Orbits at 9 January 1969
Circular and Eccentric Orbits Perturbed Only by the Aspherical Moon

Initial Orbital Elements in Selenographic System					Perturbations of the Orbit					
a	e	i	γ	ω	ΔT	Δa	Δa_m	e_{max}	Δi_E	$\Delta \Omega_E$
1788 km	0	0° 0	0° 0	0° 0	1.463 km	0.4193 km	0.0008 km	7.806×10^{-4}	0° 003552	0° 01076
1788	0	90° 0	0° 0	0° 0	1.1623	1.264	0.0049	5.474×10^{-4}	1° 167	0° 2307
1788	0	90° 0	90° 0	0° 0	0.5747	1.259	0.0091	4.345×10^{-4}	1° 116	0° 5117
2038	0	90° 0	0° 0	0° 0	0.9997	1.1051	0.0038	4.177×10^{-4}	0° 7379	0° 09893
2263	0.2098	5°	0	0	947.7381	0.9472	.2439	.2098	0° 07507	1° 8741
2263	0.2098	90°	0	0	948.4501	1.7777	.2638	.2098	0° 5605	0° 06090